6
Recent Advances in Ion Exchange Membranes for Desalination Applications

Chalida Klaysom, Bradley P. Ladewig, Gao Qing Max Lu, and Lianzhou Wang

6.1
Introduction

Ion exchange membranes (IEMs) have gained enormous attention over the past several decades because of their versatile applications in many important areas including energy and alternative clean energy, potable water production, wastewater treatment, food industry, and chemical industry [1–10]. Therefore, a solid understanding of IEMs in both material synthesis and principle theories of transport phenomena is of crucial importance for the rational development of the desired IEMs for various applications.

In this chapter, a comprehensive overview of IEMs covering the fundamentals, as well as the recent development of IEMs and their applications is provided. Although the main focus will be on IEMs for desalination application by electro-driven processes, the general concepts for developing IEMs suitable for different applications are also briefly summarized. The outline of this chapter is as follows:

1) the fundamentals of IEMs and their transport phenomena
2) the material development
3) the future perspective of IEMs.

6.2
Fundamentals of IEMs and Their Transport Phenomena

IEMs are selective membranes carrying the anionic or cationic charged groups that allow specific charged species to pass through, while rejecting others of the same charges as the membranes. On the basis of the processes the IEMs are applied to, they can be classified into three major types [11]:

- Separation processes involving the separation of a component from an electrolyte solution. They can be further subdivided based on the driving force for the transport of ionic species, such as electro-driven processes in electrodialysis (ED) and concentration gradient in dialysis or Donnan dialysis [2, 4, 6, 12, 13].

Functional Nanostructured Materials and Membranes for Water Treatment, First Edition.
Edited by Mikel Duke, Dongyuan Zhao, and Raphael Semiat.

- Electrochemical reaction, in which a certain chemical is generated such as in chloride-alkaline process [1, 2, 14].
- Energy conversion devices for applications, such as fuel cells and batteries [2, 8, 15, 16].

To date, ED and fuel cells are the most important processes using IEMs. Because IEMs have been widely used in many applications, the properties required for the IEMs highly depend on the specific application. However, generic property requirements are (i) low ionic resistance, (ii) high transport number of counterions, (iii) high selectivity, and (iv) good thermal, mechanical, and chemical stability [17].

According to the charged functional groups of membranes, the IEMs are generally subdivided into cation exchange membranes (CEMs), anion exchange membranes (AEMs), and bipolar membranes (BMs). The BMs are the membranes having layers of CEM and AEM which are adjacent and laminated together. The CEMs with negatively charged functional groups are selective to cationic species and reject anionic species and vice versa for the AEMs. The definition of the Donnan exclusion is well known as the prevention of ions with the same charges as that of the membrane to transport through the membrane by electric repulsion. On the basis of the electroneutrality, fixed charges of the membrane are neutralized and filled with its counterions, making co-ions unable to freely move through an IEM. However, in an IEM containing large pores that are charge balanced and fully filled with electrolyte solution, the Donnan exclusion can be suppressed and thus results in less selective membranes. In addition, Donnan exclusion depends on several parameters such as the concentration of fixed ions, the concentration of electrolytes, and the interaction among charge functional groups of IEMs and their counterions [18].

Ion selectivity of IEMs is quantitatively expressed in terms of membrane permselectivity, which measures the ease with which the counterion migration occurs through an IEM compared to the co-ions, and is defined as [19, 20]:

$$P_s = \frac{t_i^m - t_i}{1 - t_i} \tag{6.1}$$

where P_s is the permselectivity of IEMs, t_i^m is the transport number of the counterion in the membrane, and t_i is that of the same ion in free solution at the same concentration. The term *transport number* refers to the fraction of total current carried by counter ions through an IEM (normally more than 0.9). In addition, the selectivity of an IEM may be represented in terms of permeated equivalent of the particular ion relative to NaCl, which is the major component of nearly all natural saline water. For example, the transport number of a cation relative to sodium is defined as follows:

$$P_{Na}^{M} = \frac{t_M^m / t_{Na}^m}{C_M / C_{Na}} \tag{6.2}$$

where P_{Na}^{M} is the permeated equivalent of cation relative to sodium ion, t_M^m is the transport number of cations through membranes, t_{Na}^m is the transport number of

sodium ion through membranes, and C_M and C_{Na} are the concentration of the cation and the sodium ion, respectively. A similar expression is also used for anions relative to the chloride ion.

6.2.1 Ion Transport through IEMs

The Nernst–Planck flux equation is one of the most widely used equations for describing transport phenomena in both solution and IEMs because of its relatively simple relation. The Nernst–Planck equation is based on the assumption of the independent migration of cations and anions in solution and membranes. Although the ions in solution are treated as an independent compartment, the electroneutrality has to be balanced in which there are no excess charges in the system. The transport of ions can be expressed in terms of diffusion, migration, and convection as defined by the following equations:

$$J_i = J_{i(\mathrm{d})} + J_{i(\mathrm{m})} + J_{i(\mathrm{con}v)} \tag{6.3}$$

$$J_i = D_i \frac{\mathrm{d}C_i}{\mathrm{d}x} - \frac{z_i F C_i D_i}{RT} \frac{\mathrm{d}\varphi}{\mathrm{d}x} + vC_i \tag{6.4}$$

where J_i is the flux of component i, v the velocity, C the concentration, D the diffusion coefficient, x the direction coordinate, z the valence charge, F the Faraday constant, R the gas constant, T the temperature, and φ the electrical potential. Furthermore, these forms are defined as follows:

- *Diffusion* is the movement of molecular components caused by chemical potential gradient. In the IEM system, the dominant term for ion movement by diffusion is the concentration gradient.
- *Migration* is the movement of ions due to an electrical potential gradient, which is normally developed by the application of external power source.
- *Convection* is the movement of mass caused by mechanical force such as hydrodynamic flow or stirring. This term is normally of less importance in the solid membrane and can be neglected in the system when there is no flow or strong stirring condition.

The Nernst–Planck model neglects the factor of interaction among different ions and solvents in the real situation. Consequently, the irreversible thermodynamic approach, which takes the effects of fluxes of heat, electricity, momentum, and interaction among individual components and solvents into account, is considered more reasonable and practical to apply in the real system. In this section, the only basic properties and phenomena of ion exchange capacity (IEC) are presented. The detailed explanation for the transport phenomena in membranes can be acquired from the literature [17, 20–26].

6.2.2 Concentration Polarization and Limiting Current Density

Owing to the difference in ion mobility in selective membranes and in electrolyte solution, a decrease in electrolyte concentration takes place near one side of the membrane surface and the accumulation takes place on the other side of the surface. As a result, the concentration gradient develops near the membrane surface, referring to concentration polarization.

As a consequence of the concentration polarization development, if the concentration exceeds the solubility limits, precipitation will occur in the concentrate compartment. The scale on the membrane surface creates an extra resistance and can damage the membranes. In the dilute compartment, when the ion concentration near the membrane interface reaches zero there is a drastic increase in the resistance and potential drop across the membrane, resulting in high energy consumption and enhanced water dissociation. The water dissociation has dramatic effects on the electro-driven process, responsible for the loss of current utilization and undesirable consequences from the pH changes. The increased pH of solution near the CEMs' interface in the concentrated cell further enhances the precipitation and scaling phenomena. In contrast, the decreased pH of the solution near the AEM can damage the membranes. Therefore, the concentration polarization effects are required to be minimized especially to avoid water dissociation phenomena.

The concentration polarization can be reduced by reducing the current density and the thickness of its boundary layer near the membrane interface. The thickness of the boundary layer is determined by the hydrodynamic flow, which depends on the cell and spacer design and the feed flow velocity. At the provided constant velocity, the current density will reach the maximum value when salt concentration near the membrane interface in the depleting solution is reduced to nearly zero. This maximum current density is called limiting current density (LCD), and can be defined by the following equation based on the classical polarization theory:

$$i_{\text{lim}} = \frac{FDC}{z\delta\left(t_i - t_i\right)} \tag{6.5}$$

where i_{lim} is the LCD and δ is the diffusion boundary layer. The definitions of F, D, and C can be found in Equation 6.4. In practical ED, the operating condition of the system is limited by the LCD. It was believed that operating the ED over the LCD leads to the reduction of current efficiency and other unpredictable phenomena such as the scaling on the membrane surface.

6.2.2.1 The Overlimiting Current Density

On the basis of classical polarization, there are no more ions to transport and thus no current that exceeds the limiting current. However, in practice, current density over the limiting current is normally observed. In the past, it was believed that the water dissociation is responsible for the overlimiting current density as the OH− and H+ that can migrate through the membrane and carry the current are

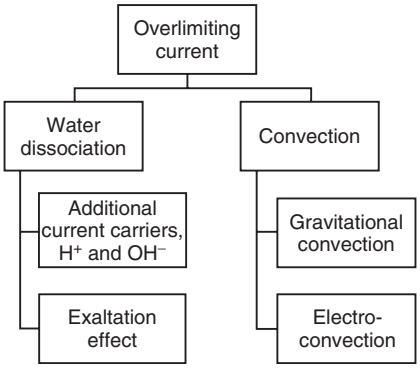

Figure 6.1 Scheme of the mechanism for overlimiting current transfer.

generated. However, it has been demonstrated and reported in several experimental studies that the water dissociation is not responsible for the origin of overlimiting current [20, 23, 27–39]. The transport of OH− and H+ only partly contributes to the current over the limiting current. The origin of the current over the limiting one is still unclear and is now a subject of intensive discussion [20, 23, 27–39].

To date, several models have been developed to describe the mechanism of overlimiting current for a better understanding of its phenomena and its role in an application, consequently leading to the design of membranes that can overcome or minimize the effects of concentration polarization phenomena. The state-of-the-art mechanism describing the origin of overlimiting current by coupled effects is summarized in Figure 6.1 [23, 25, 28].

6.2.2.2 **Water Dissociation**

The water dissociation is generally expressed by Equation 6.6.

$$H_2O \rightleftarrows H^+ + OH \tag{6.6}$$

In IEMs, the water splitting reaction occurs within a thin layer near the membrane interface in the depleting side. It was found that the water splitting in electrodriving membrane processes is higher than that in normal water solution, as the fixed charge groups of the IEMs can also be involved in the reaction as catalysts [23, 25, 28]. Nikonenko *et al*. [23] reported the range of ionic functional groups of IEMs in the order of increasing water dissociation as shown below:

$$-N^+(CH_3)_3 < -SO_3^- < -PO_3H < =NH, -NH_2^+ < -COO^- < -PO_3^{2-}$$

In addition, water dissociation becomes more rapid with the presence of metallic hydroxides such as $Mg(OH)_2$, and $Fe(OH)_3$, which are normally precipitated on the CEM surface and act as a catalyst for the water dissociation reaction [23, 25, 29].

The counterion transfer can also be increased with the occurrence of water splitting; the generated H+ or OH− near the membrane surface attracts the ions from the adjacent bulk solution toward the membranes (an exaltation effect) [28]. For example, the OH− near CEM surface attracts cations from the bulk depleting

solution toward the boundary layer near the membrane surface, resulting in the increase of ions to transport through the membranes.

6.2.2.3 Gravitational Convection

Gravitational convection provides additional counterion transfer by the enhancement of solution mixing. This type of convection is developed because of nonuniform distribution of temperature or solution density near the membrane interface [40]. The high resistance that develops on the dilute side because of concentration polarization, can lead to Joulean heat production and the formation of a temperature gradient. The concentration density and temperature gradient correspond to the mixing and movement of the counterion, contributing to the overlimiting current [40].

Many research studies have investigated the effect of natural convection and the gravitational convection by mounting membranes in two different configurations, vertical and horizontal position [23, 28, 30, 33, 35, 40–44]. It has been proved that when membrane is rearranged in the horizontal position with the dilute compartment underneath the membrane, the gravitational diffusion layer is stabilized and the free convection is minimized. In that case, the counterions that transfer under the influence of convection are neglected. The current over the limiting value was still observed in this case; implying that the transport of the ions may be contributed by the gravitational convection and may also be coupled by other phenomena, such as electroconvection.

6.2.2.4 Electroconvection

Electroconvection is due to the nonuniform electric field near the membrane surface, which causes the turbulent movement in the boundary layer and the transport of counterions. This phenomenon is highly influenced by the surface inhomogeneity of the membranes and more pronounced in the depleting solution. The mechanism governing the electroconvection in a membrane is believed to be electroosmotic slip of second kind or ''electroosmosis II'' referring to the occurence of electroosmosis due to an interaction between an electric field and the induced space charge near the membrane interface in the diffusion boundary layer [35]. The strength of the electric field is likely to be dependent on the Strokes radius of ions of the space charge layers. The larger the Stroke radius the stronger the space charge layer, contributing to the electroconvection and the enhancement of liquid motion [43].

6.2.3 Structure and Surface Heterogeneity of IEMs

Bulk and surface morphologies of IEMs play an important role on the membranes' properties, especially on the electrochemical properties and transport phenomena of the membranes.

The inner membrane morphology (bulk morphology) determines, to a large extent, the electrical conductivity, transport phenomena, permselectivity, diffusion,

and hydraulic permeability of the IEMs. A microheterogeneous model is normally used for describing the transport characteristics of membranes in particular to measure the degree of membrane structural heterogeneity and correlate with membrane electrochemical behavior [32, 45, 46]. In the microheterogeneous model of IEMs, an IEM consists of a gel phase and intergel phase of filling solution. The gel phase is composed of fixed charged functional groups, which are considered to have a relatively uniform distribution on polymer chains and compensated solution of the fixed charged functional groups (Figure 6.2).

Many works also referred to a two-phase model that combines volume fraction of the inert phase into the gel phase and considered them as a quasi-homogeneous region, namely joint-gel phase. The use of two-phase model to explain the electrochemical behavior of various commercial IEMs was reported [32, 45]. They concluded that the selectivity of IEMs depends on the volume fraction of joint-gel phase and intergel phase. As the volume fraction of the intergel phase that is considered as the nonconducting region increases, the Donnan exclusion becomes less effective and thus results in a less selective membrane. When three different electrolyte solutions were used, it was found that the fraction of the intergel phase was considerably independent to the electrolyte solution. Therefore, the fraction of intergel phase was concluded to directly relate to the morphology of tested membranes and independent to the electrolyte solution [45].

The surface heterogeneity of the IEMs has been intensively investigated recently, mostly by chronopotentiometry and current voltage (i–v) characteristics [30–33, 40, 46]. Chronopotentiometry is a powerful characterization technique that measures the correspondent potential of a system imposed to constant current. It has been widely applied for investigating the transport phenomena of the IEM, especially in the diffusion-controlled boundary layers to better understand the overlimiting current behavior of a membrane [30, 33, 40, 43, 47, 48]. The shapes and characteristic values of chronopotentiograms depend on many parameters such as membrane resistance, surface and structure properties of membranes, the testing, and the hydrodynamic conditions [40]. The typical shape of a chronopotentiogram is presented in Figure 6.3.

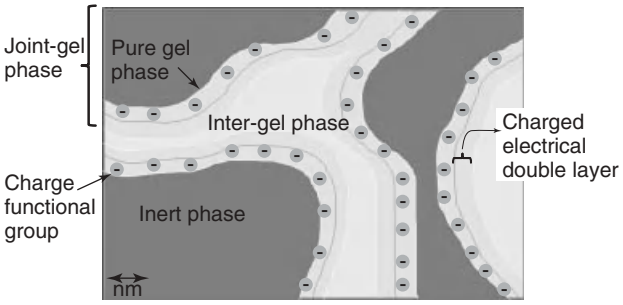

Figure 6.2 Scheme representative structure of IEM according to the micro-heterogeneous model. (Source: Adapted from C. Larchet *et al*. [43].)

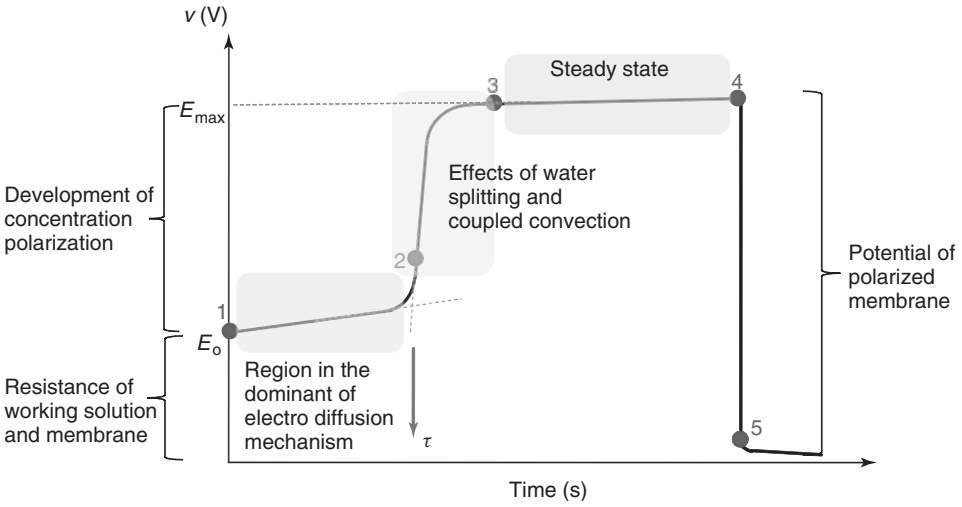

Figure 6.3 A representative chronopotentiogram of IEM.

When a constant current density is applied to the testing cell, the initial potential difference (E_o) is suddenly built up; its height is related to ohmic potentials of the resistance of the testing system (electrolyte and membrane). The potential difference gradually increases as a function of time because of the gradual increase in ohmic resistance of the system (region I from point 1 to 2). The slope of this part depends on the capacity of the charged electrical double layer at the membrane interface. The transport phenomenon of this region is governed mainly by electrodiffusion process. When the concentration of the depleting solution near the membrane interface reaches zero, suddenly the sharp developed potentials occur (at the infection point (2)). The transport mechanism of the IEMs changes mainly to a coupled convection. After that the curve reaches the steady state where the potential difference levels off (E_{max}). Note that the transition point can only be observed when the current higher than the LCD is applied to drive the change of transport phenomena on the membrane surface from electrodiffusion to other mechanisms. The difference between the initial potential and the potential at steady state (ΔE) indirectly relate to the thickness of concentration gradient [47]. Under the concentration polarization theory, the better the transport property the membrane is, the larger ΔE will be observed. As membranes with high transport property can transport ionic species from one side to the other better than the membranes with lower transport property, the ΔE between its two interfaces is thus bigger.

The i–v characteristic is another useful technique to investigate the concentration polarization of membrane interface and the LCD. Typically, the shape of i–v curve depends on the nature and surface properties of the membranes, the property of electrolyte solution, and the hydrodynamic condition in the testing process [30, 37, 38, 49, 50]. This technique records the corresponding current density with

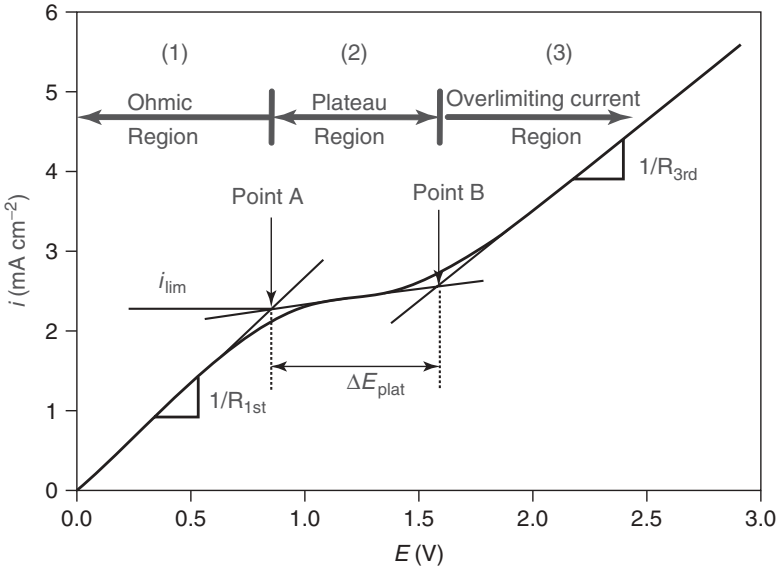

Figure 6.4 The representative characteristic i–v curve.

the stepwise potential difference. Typically, an i–v curve can be divided into three regions, as shown in Figure 6.4.

The region (1), the Ohmic region, is the region where the current density is linearly proportional to potential difference. When the ion concentration in the boundary layer near membrane interface decreases toward zero and there are a limited number of ions that can carry the current, the current reaches the plateau range in that region (2). The LCD occurs at the inflection point that can be estimated from intersection of the tangents between region (1) and (2). The corresponding current above the plateau region can be referred to a overlimiting current region (region (3)), which is believed to be influenced dominantly by the coupled convection effect.

It was found that surface heterogeneity of the membranes has a high impact on the membrane electrochemical behavior and the development of concentration polarization. Specifically, the presence of nonconducting regions reduces the active transfer areas, resulting in locally higher current density near the conducting regions compared to the overall current density across entire membrane area (Figure 6.5). This phenomenon has a strong influence on the characteristic curves of chronopotentiograms and i–v curve, as shown in Figure 6.6a,b.

Membranes with homogeneous and heterogeneous surfaces obtained different characteristic curves in a chronopotentiogram (Figure 6.6a). While heterogeneous membranes gave a shorter transition time and more diffuse curve near the inflection region, the more homogeneous membranes possess longer transition times and almost vertical curve from inflection point to the steady state [51]. This is due to the nonuniform current line distribution of the heterogeneous membranes. As

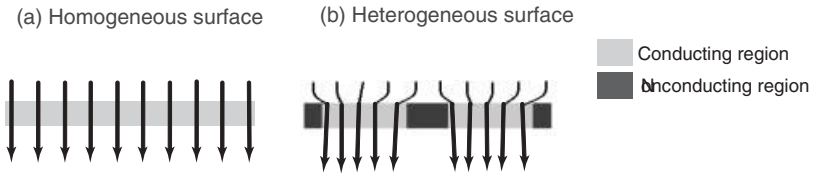

Figure 6.5 Current line distribution through (a) homogeneous surface and (b) heterogeneous surface of ion exchange membranes.

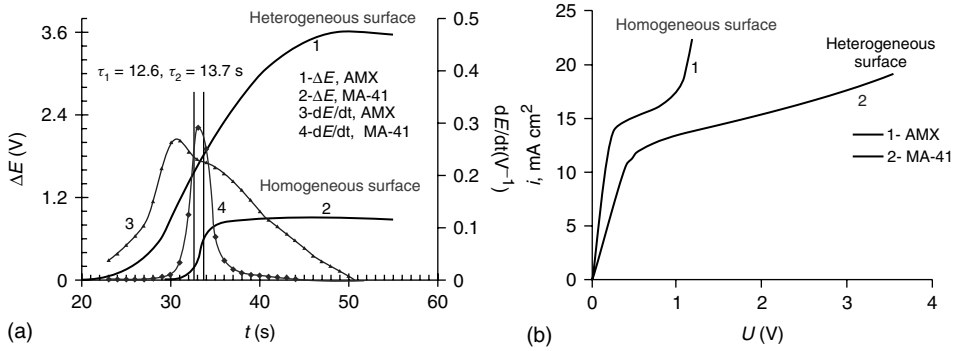

Figure 6.6 Different shapes and characteristic curves of homogeneous and heterogeneous commercial membranes (AMX from Tokuyama Soda and MA-41 from Schekino Production): (a) chronopotentiograms and their derivatives of a homogeneous AMX and a heterogeneous MA-41 and (b) i–v curve of AMX and MA-41 membrane. (Source: Adapted from N. Pismenkaia *et al.* [40]).

in the heterogeneous membrane, the local LCD near the conducting region is higher than the average current density of the whole surface, the ionic species are removed faster and thus the concentration decreases quickly and the potential difference develops rapidly at the beginning of the process, resulting in reaching the transition time sooner. Furthermore, the time the heterogeneous membranes required to achieve a quasi-steady state is slower compared to a more homogeneous one as the slow growth of the potential drop is observed from the inflection point.

The degree of surface heterogeneity also has a strong impact on the i–v development of the concentration polarization visible in the i–v curves (Figure 6.6b) [52]. It was found that the lower LCD was obtained in the case of heterogeneous membranes. Balster *et al.* [27] also studied the cause and phenomena of the overlimiting current using microheterogeneity model and microtopology technique. They concluded that surface heterogeneity of membranes has a great influence on the shape of the i–v curve and its plateau length. In general, the more heterogeneous the membrane surface the longer the plateau length. If the space distance between the conducting and nonconducting regions is in the same magnitude with the boundary-layer thickness, the shortening of plateau length can normally be observed.

6.3
Material Development

This section provides an overview of the progress in the development of IEMs, including the various approaches made to the membrane modification. Various types of IEMs have been developed for different applications. Some commercial IEMs, manufacturers, and their properties are shown in Table 6.1 [18, 53, 54].

6.3.1
The Development of Polymer-Based IEMs

The search for new materials for IEMs has kept intensifying in order to supply robust membranes for the existing applications and to expand the opportunity to new potential applications. Polymer IEMs can be prepared via three approaches depending on the starting materials.

1) Introduction of charged moieties to polymer chains followed by the formation of membranes.
2) Polymerization of monomers containing charged moieties. The charged polymers then undergo film processing to form membranes.
3) Introduction of functional charged groups on the already film-formed membranes.

6.3.1.1 Direct Modification of Polymer Backbone

Polyarylene polymers containing aromatic pendant groups on polymer backbones such as poly aryl sulfone, poly aryl ketone, polybenzimidazole (PBI), polyphenylquinoxalines (PPQs), and polyphenylene oxides (PPOs) are attractive as new polymer matrix for IEMs due to several reasons: (i) their mechanical and thermal stability, (ii) processibility, (iii) low cost, and last but not the least, (iv) the ability to chemically modify the polymer backbone via the electrophilic substitution at their aromatic skeletons [55–59]. The introduction of charged moieties by direct polymer backbone modification via the electrophillic substitution is widely used owing to its simplicity and reproducibility under defined conditions [59].

Poly(aryl sulfone) Thermoplastic poly (aryl sulfone) such as polyether sulfone (PES) is one of the most widely studied polymers because of its excellent mechanical, thermal, and chemical stability. Moreover, PES possesses a high degree of process flexibility [60]. A number of research projects have focused on the development of PES as IEMs to replace expensive Nafion membranes. This type of polymer has been prepared with various structures, referring to slightly different pendent groups in the polymer back bones (as shown in Figure 6.7), available from different suppliers. Consequently, there are several ways to introduce charged functional groups (predominantly sulfonate groups ($-SO_3H$)) into the polymer backbones. Table 6.2 provides different path ways of the electrophillic substitution reactions applied to different PES structures.

Table 6.1 Properties of some commercial IEMs.

Membrane	Type	Thickness (mm)	Water content (%)	Area resistance (Ω cm^{-2})[a]	IEC (mequiv g^{-1})	Permselectivity (%)[b]
Tokuyama Soda Co. Ltd, Japan						
Neosepta CMX	CEM, PS/DVB	0.14–0.20	25–30	1.8–3.8	1.5–1.8	97
Neosepta AMX	AEM, PS/DVB	0.12–0.18	25–30	2.0–3.5	1.4–1.7	95
Neosepta CMS	CEM, PS/DVB	0.15	38	1.5–2.5	2.0	—
Neosepta ACM	AEM, PS/DVB	0.12	15	4.0–5.0	1.5	—
Asahi Glass Co. Ltd, Japan						
CMV	CEM, PS/DVB	0.15	25	2.9	2.4	95
AMV	AEM, PS/BTD	0.14	19	2.0–4.5	1.9	92
HJC	CEM, heterogeneous	0.83	51	—	1.8	—
Ionic Inc., USA						
61CZL386	CEM, heterogeneous	0.63	40	9	2.6	—
103PZL183	AEM, heterogeneous	0.60	38	4.9	1.2	—
Dupont Co., USA						
Nafion 117	CEM, fluorinated	0.20	16	1.5	0.9	97
Nafion 901	CEM, fluorinated	0.40	5	3.8	1.1	96
RAI Research Corp., USA						
R-5010-H	CEM, LDPE	0.24	20	8.0–12.0	0.9	95
R-5030-L	AEM, LDPE	0.24	30	4.0–7.0	1.0	83
R-1010	CEM, fluorinated	0.10	20	0.2–0.4	1.2	86
R-1030	AEM, fluorinated	0.10	10	0.7–1.5	1.0	81
CSMCRI, Bhavangar India						
IPC	CEM, LDPE/HDPE	0.14–0.16	25	1.5–2	1.4	97
IPA	AEM, LDPE/HDPE	0.16–0.18	15	2.0–4.0	0.8–0.9	92
HGC	CEM, PVC	0.22–0.25	14	4.0–6.0	0.7–0.8	87
HGA	AEM, PVC	0.22–0.25	12	5.0–7.0	0.4–0.5	82

Table 6.1 (*continued*).

Membrane	Type	Thickness (mm)	Water content (%)	Area resistance (Ω cm^{-2})[a]	IEC (mequiv g^{-1})	Permselectivity (%)[b]
FuMa-Tech GmbH, Germany						
FKE	CEM, —	0.05–0.07	—	<3	>1	>98
FTCM-A	CEM, PA	0.50–0.60	—	<10	>2.2	>95
FTCM-E	CEM, PET	0.50–0.60	—	<10	>2.2	>95
FAD	AEM, —	0.08–0.10	—	<0.8	>1.5	>91
FTAM-A	AEM, PA	0.50–0.60	—	<8	>1.7	>92
FTAM-E	AEM, PET	0.50–0.60	—	<8	>1.7	>92

[a]Measured: 0.5 mol dm^{-3} NaCl and
[b]0.1/0.01 mol dm^{-3} NaCl and 0.1/0.5 mol dm^{-3} KCl for membranes from FuMa-Tech GMbH at 25 °C.

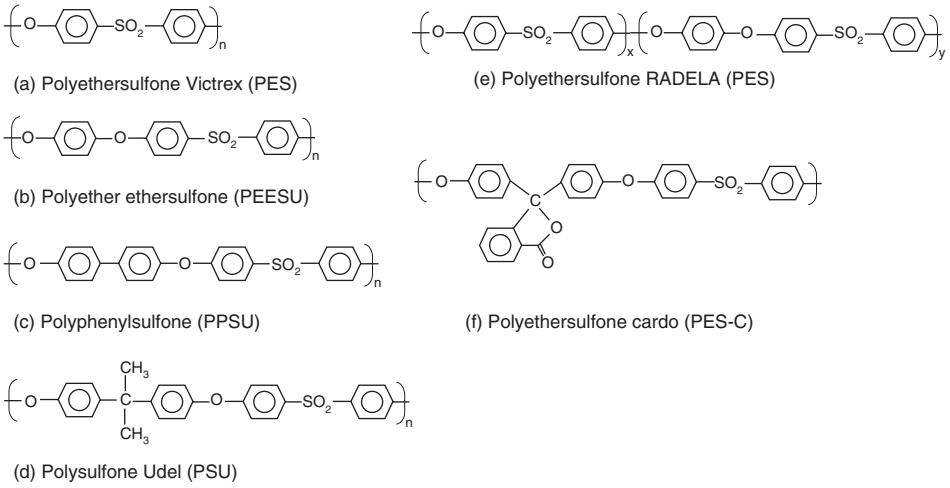

Figure 6.7 Different chemical structures of poly (aryl sulfone) base polymers.

The AEM based on PES can also be prepared by conventional chloromethylation and quaterамination [69, 70]. Although the resultant AEM showed high ionic conductivity and good IEC, which is an expression of the equivalent number of fixed charge groups per unit of dry membrane weight, the chloromethylation step requires the use of toxic solvent of chloromethylether that can be harmful to human health.

Poly(aryl ether ketone) The polymer family of poly (aryl ether ketone) has also been intensively studied recently [8, 59, 71–78]. The modification of the polymer backbone can be carried out in the same manner as for PES polymer family.

Table 6.2 Sulfonation reaction for PES polymers.

Sulfonation reagent/process	Polymer	Solvent	Note
Chlorosulfonic acid [58, 60–64]	PES	H_2SO_4, Chloroform, Dichloromethane (DCM), Dichloroethane (DCE)	• Simplicity • Difficulty for the chemical disposal of concentrated H_2SO_4 acid • Hard to control the undesirable side reaction
Methylation-sulfonation-reaction [65, 66]	PSU	*N*-methyl pyrolidone (NMP)	• Good quantitative and region-specific reaction control • Complicated procedure
Sulfurtrioxide triethyl phosphate (SO_3-TEP) [67, 68]	PES	DCM	• Minimize or eliminate the possible side reactions • Convenient and relatively inexpensive • Difficult to control the sulfonation reaction to a specific stable position

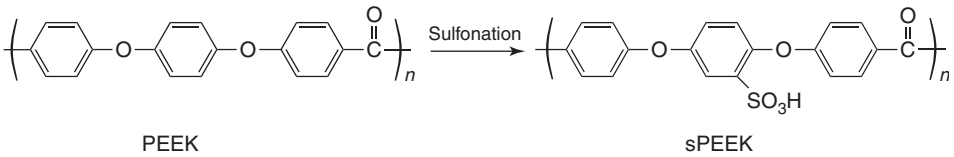

Figure 6.8 Chemical structures of polyether ether ketone(PEEK) and sulfonated polyether ether ketone (sPEEK).

Figure 6.8 depicts the chemical structure of poly (ether ether ketone) (PEEK, Victrex) and the sulfonated poly (ether ether ketone) (sPEEK).

The most commonly used method for preparation of CEM from PEEK is by dissolving the polymer in H_2SO_4 acid [71, 73, 74]. The sPEEK with the degree of sulfonation (DS) of around 90% showed a high IEC of 2.48 mequiv g^{-1} with similar proton conductivity of Nafion. However, it is worth noting that the resultant sPEEK with the high DS exhibited poor thermal stability that makes it difficult for the fabrication into membrane films in melt processes [72]. Moreover, sPEEK with the high DS can uptake water molecules up to four molecules per sulfonate group and increase the number of water uptake up to eight molecules per unit functional group when it was formed in the films, resulting in high degree of water swollen and poor dimensional stability. This poor melt processibility and dimensional

stability limited the application of the sPEEK. Therefore, much effort has been focused on the strategies to overcome the aforementioned problems of the sPEEK. Blending the sPEEK with other polymers or the introduction of cross-linking agents to the sPEEK are powerful strategies to improve the poor thermal and mechanical stability of the sPEEK membrane. The sPEEK can also be cross-linked either by reaction bonding or thermal treatment to improve the dimensional stability of membranes [79].

Polyphenylene Oxides (PPO) AEMs based on the PPO have been prepared either by chloroacetylation and quaternary amination or by bromination and amination processes [80–83]. Also, CEMs can be prepared by the same strategy of bromination and then sulfonation reaction as shown in Figure 6.9 [59, 84].

The new path way for preparing AEMs as proposed in the Figure 6.9 provides an advantage of avoiding the use of toxic chemical such as chloromethyl methylether, normally used in the conventional preparation procedure of AEMs. Via the approach illustrated in Figure 6.9a, the membranes with high IEC can be obtained. However, the thermal stability of the resultant membranes still requires more improvement. This problem can be solved by the introduction of bromination substitution (Figure 6.9b), which can occur on both aryl and benzyl position. As a consequence, the amination can occur in both positions and can also create cross-linking to some extend among the functional groups of the membranes. It has been reported that the position of the moieties groups has a high influence on the properties of the resultant membrane [80]. The balance of the functional groups on benzyl and aryl position allows the tuning of membrane properties, desirable for different application needs.

6.3.1.2 Direct Polymerization from Monomer Units

The direct synthesis of polymer from monomer units provides excellent opportunity in tailoring polymer composition that allows the control of amount and distribution of the ionogenic functional groups along the polymer backbones. This also advances the tuning of both microstructure and properties of the IEMs.

Polyethersulfone (PES) The direct polymerization from monomer units offers some advantages on the precise control of sulfonate groups on the aromatic rings of the polymer backbones, and the feasibility to tune the molecular weight of the polymer, thus leading to the polymer with higher mechanical stability and better processibility.

The sulfonated polyethersulfone (sPES) via direct polymerization of monomers containing charge moieties have been successfully reported [85–90]. In practice, sPES can be obtained by the direct aromatic nucleophilic substitution and polycondensation of dichlorodiphenylsulfone (DCDPS), 3,3′-disulfonate dichlorodiphenylsulfone (SDCDPS), and biphenol as shown in the Figure 6.10.

The resultant membrane based on sPES obtained from direct polymerization of the monomer units exhibited high IEC up to around 3 mequiv g^{-1}. However, at high DS, the membranes suffer from high swollen degree, resulting in low

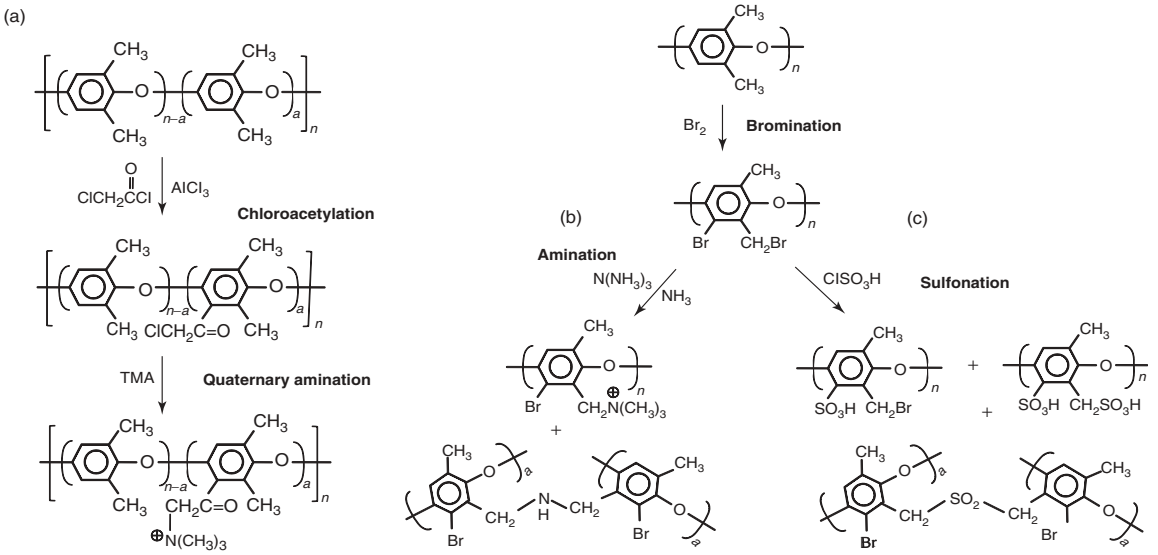

Figure 6.9 Main reactions and structures of IEMs from PPO: (a) anion exchange membranes employing Friedel-Crafts chloroacetylation, (b) anion exchange membrane prepared by bromination and amination, and (c) cation exchange membrane prepared by bromination and sulfonation reaction.

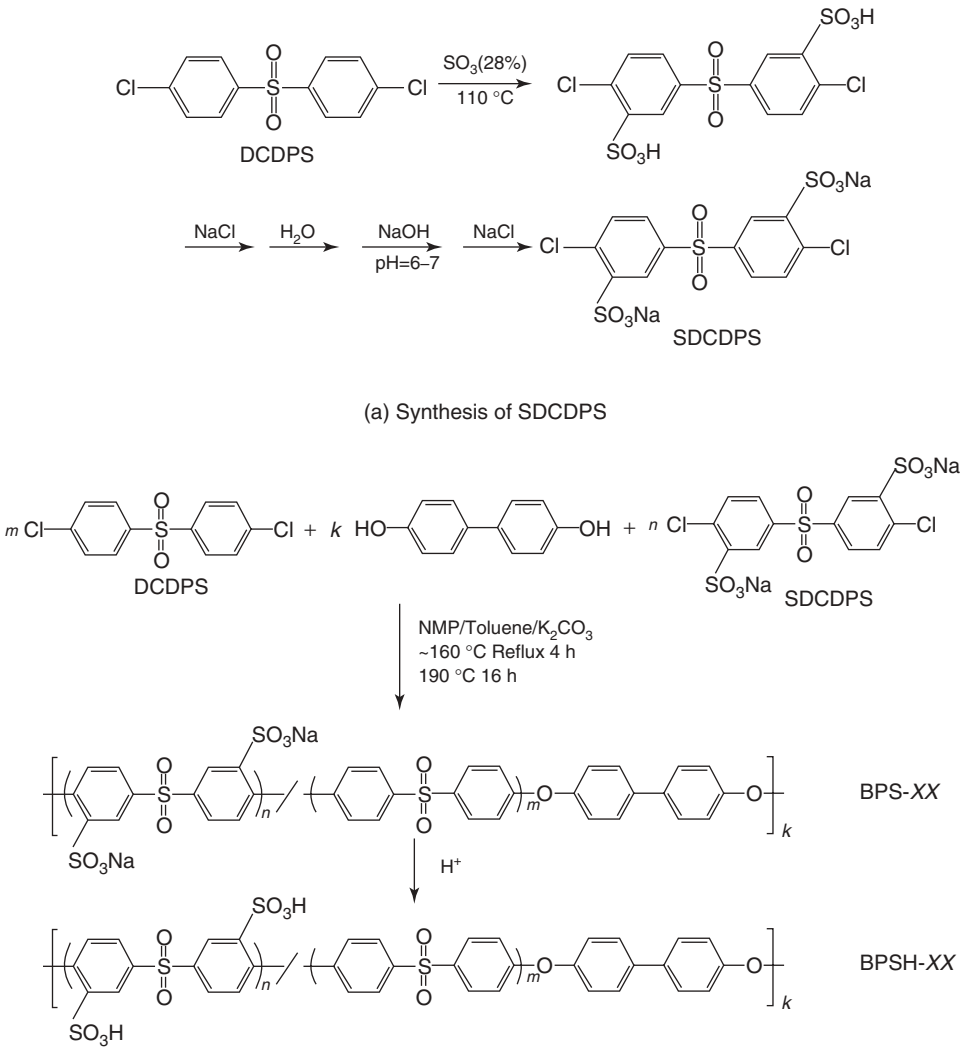

Figure 6.10 (a) Synthesis of sDCDPS and (b) sulfonated poly (arylene ether sulfone).

mechanical stability. To improve the dimensional stability of the membrane, a certain degree of cross-linking was introduced [55]. The cross-linked membranes can have significantly improved mechanical stability, while still maintaining good conductivity.

6.3.1.3 Charge Induced on the Film Membranes

The IEM can also be prepared by forming the non-ionogenic polymer films first, and subsequently by the introduction of charged functional groups onto the formed polymer films.

The radiation-induced grafting is a versatile technique to introduce functional groups onto different membrane substrates [91, 92]. The grafting technique offers several advantages to the membrane development, including feasibility in processes, well-defined composition, and ability to tailor membrane properties with a variety material selection, including surface substrates, grafting materials, and induced functionalities [91, 93]. The film substrates can be porous or nonporous membranes. Typical examples include hydrocarbon polymer-based films of polyethylene (PE), polypropylene (PP), polyalkene (polyalkene nonwoven fabrics (PNF)), and fluorocarbon polymer-based films of polyvinylidene fluoride (PVDF), polytetrafluoroethylene (PTFE), poly(tetrafluoroethylene-*co*-hexafluoropropylene) (FEP), and poly(ethylene-*co*-tetrafluoroethylene) (ETFE) [15, 16, 94–97]. The chemically stable fluorinated carbon films are normally selected for applications that require robust membranes to withstand severe working conditions [98, 99]. For the grafting agents, there are two major types: (i) functional monomers such as acrylic acid and methacrylic acid that can be attached directly to the substrate as charged functional groups and (ii) nonfunctional monomers such as styrene, *N*-vinylpyridine, and vinylbenzylchloride that can be further chemically modified or conversed into ion exchangeable groups.

CEMs with carboxylic acid functional groups (–COOH) can be prepared by either direct grafting of acrylic monomers or by indirect grafting of epoxy acrylate monomers on the polymer films (PE, PNF), followed by postgrafting treatment with sodium iminodiacetate [95, 98]. The membranes with sulfonated groups ($-SO_3H$) are normally prepared by grafting polymer films (PE, FEP, PNF, or PTFE) with styrene and subsequently sulfonating the grafted films with chlorosulfonic acid, or sulfuric acid in dichloromethane or tetrachloroethane for carbon tetrachloride solution [100–102]. It is worth noting that the nature and properties of grafted film substrate has to be taken into account when selecting the suitable sulfonating agents.

The AEMs can also be prepared in the same manner as the CEMs with sulfonate groups as depicted in Figure 6.11 [95, 103, 104]. First, vinylbenzylchloride or glycidyl methacrylate (GMA) is grafted on the film substrates (PNF), followed by amination reaction to convert the functional groups to amine derivatives.

The IEMs prepared form grafting technique showed high conductivity and good chemical, thermal, and mechanical stability which make them interesting for industrial applications. The grafting method was proved powerful as the properties of the IEMs can be conveniently controlled. However, most IEMs prepared by the grafting technique are still at a laboratory scale; the commercial success is still limited [105]. This may be due to the constrained access to the radiation source and the difficulty in the reproduction of uniformly grafted membranes

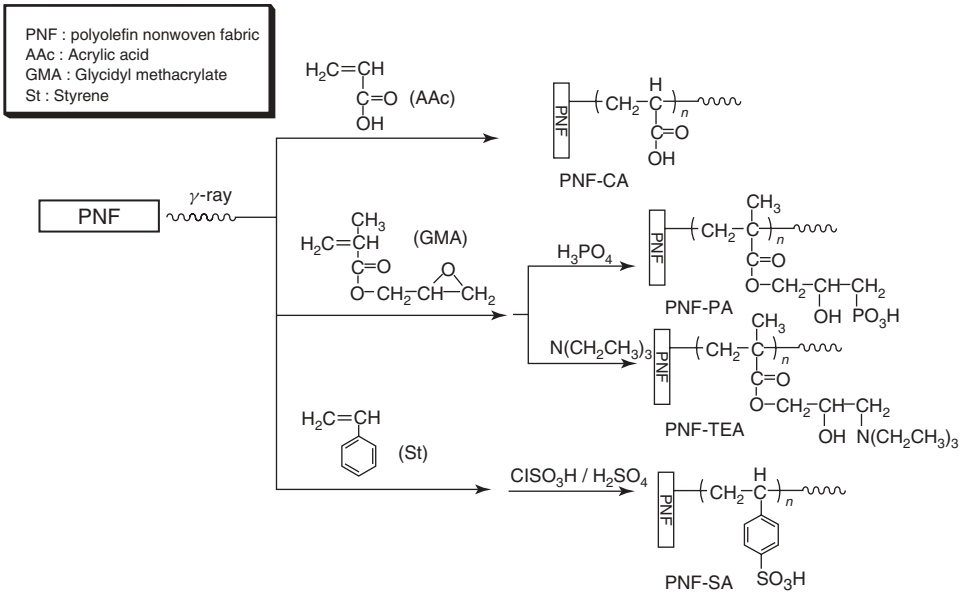

Figure 6.11 Schematic diagram for the preparation the IEM by grafting method [95].

on a large scale. This leaves big challenges for feasibility study, scale up, and commercialization.

6.3.2
Composite Ion Exchange Membranes

At this point, one can obviously notice that it is difficult to acquire all the targeted properties in one IEM to satisfy the requirements of industrial applications. For instance, to obtain high conducting membranes, high chemical modifications should be applied to the membrane, which will subsequently reduce the mechanical stability. Hence, innovative composite concept that enables the structural and functional tailoring of different materials may offer an alternative approach for the development of new IEMs with excellent electrochemical properties and good mechanical stability.

Inorganic–organic composite materials have gained increased attention because of its specific properties arising from synergistic effects among the components in the composite. The inorganic compartment usually offers vehicles for carrying extra charge functional groups, electrical properties, and enhancement of chemical, thermal, and mechanical stabilities. In contrast, the organic counterpart provides opportunities for chemical modifications, structure flexibility, and processibility on large scale.

The composite IEMs can be prepared by several routes such as sol–gel process, blending, *in situ* polymerization, molecular self-assembly [106–111]. Table 6.3 provides examples of composite IEMs prepared from different routes and their

Table 6.3 Preparation routes of composite IEMs and the resultant membrane properties.

Composite system	Preparation route	Property	Application
Nafion-silica [112–114]	Sol–gel	The composites showed significant reduction of methanol crossover, however, their proton conductivity was diminished	DMFCs
Nafion-sulfonated mesoporous silica [115]	Blending	The composite exhibited the enhanced proton conductivity and reduced methanol crossover up to 30% reduction compared to the pristine Nafion	DMFCs
PEO-$[Si(OEt)_3]_2SO_3H$ [81]	Sol–gel	• Estimated pore diameter of 1–4 nm • Thermal stability up to 265 °C • IEC of 0.4–1.0 mequiv g^{-1}	NF
sPES-silica [116]	Sol–gel	High proton conductivity of 63.6 mS cm^{-1} and good IEC comparable to Nafion, the commercial membrane	DMFCs
sPES-sulfonated mesoporous silica [117–121]	Blending	The composite showed good IEC, ionic conductivity, transport properties while maintain decent mechanical and thermal stability	ED Water splitting
PVA-zirconium phosphate [122]	Blending	• Proton conductivity of 1–10 ms cm^{-1} at 50%RH • Reduced methanol crossover	DMFCs
PVA-silica [123–125]	Sol–gel	• IEC of 0.84–1.43 mequiv g^{-1} • Proton conductivity of 20–110 mS cm^{-1} at room temperature with fully hydrated condition	Electrodriving process, DMFC
sPEK/sPEEK-SiO_2, TiO_2, ZrO_2 [126]	Sol–gel	Though the composites showed up to 60-fold reduction of methanol flux, their proton conductivity was affected by 10–30% reduction	DMFCs

Note: DMFCs, direct methanol fuel cells; NF, nano filtration; ED, electrodialysis; PVA, polyvinyl alcohol; and PEO, polyethylene oxide.

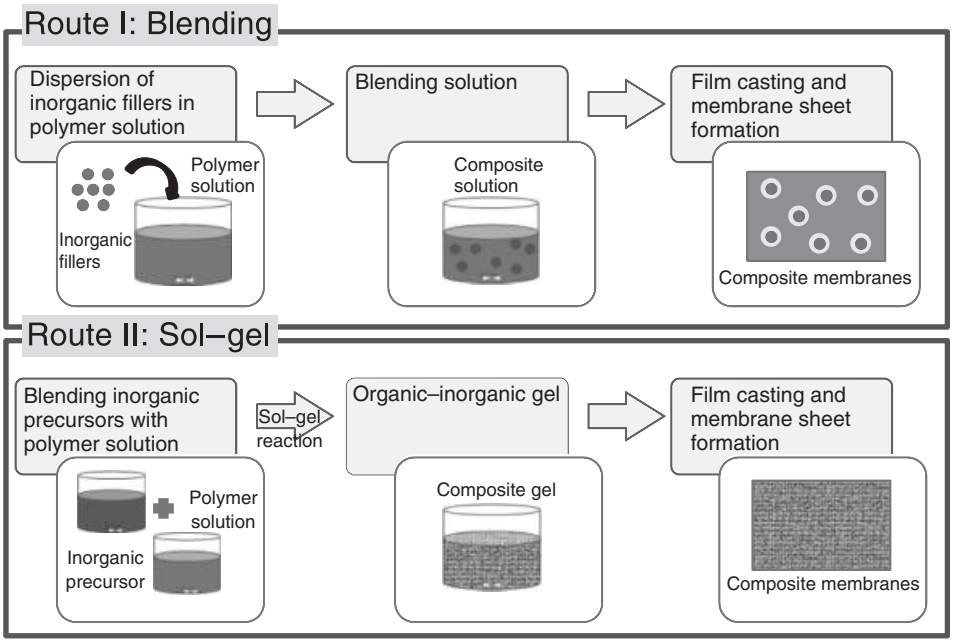

Figure 6.12 The most commonly used preparation methods for composite membranes: Route I blending and route II sol–gel method.

properties for specific applications. It is worth noting that the most frequently used routes are physical blending and sol–gel technique as depicted in Figure 6.12. For the first approach, the resultant membranes normally show phase separation from aggregated fillers, causing mechanical instability of the membranes. In contrast to the first approach, sol–gel method offers better interconnection between two domains.

The great challenges in developing composite materials are the incompatibility between the distinct compartments, aggregation of fillers, and their phase separation. However, this problem can be minimized by enhancing the interaction among them via covalent bond, hydrogen bond, and electrostatic interaction. Frequently used strategies for improving the interaction between inorganic and organic matrix are; (i) functionalization of inorganic fillers or/and polymer matrix and (ii) introduction of the inorganic filler on the polymer chains [127]. In the later case, the inorganic fillers can be fixed to the polymer by several approaches such as attaching the initiator or functional group that can further be polymerized with the polymer matrix.

As it can be noticed from Table 6.3, though the development of composite IEMs for fuel cell applications has been well established, there are very rare works applying the same composite concept to develop other types of electro-driven membrane processes [117–121].

Recently, our research group has developed a series of composite IEMs based on sPES and sulfonated mesoporous silica. By synergistic approaches of membrane preparation technique, the so-called, two-step phase inversion and the presence of surface functionalized silica nanofillers, membranes with controllable porosities and desired properties were successfully prepared. The synthesis route of these composites is depicted in Figure 6.13 [117].

The two-step phase inversion technique allows the control of membrane porosities by tuning the aging time before precipitating the partly dried film in water bath. As the viscosity and solvent/nonsolvent exchange rate altered accordingly, the pore sizes and the porosity of membrane were able to be controlled. The surface functionalized silica acted as the vehicle carrying extra charged functional groups for ion exchange, resulting in the improvement of water uptake, conductivity, transport properties, and electrochemical behavior of the resultant composites. However, at a high percent loading, the reduction of such properties was observed

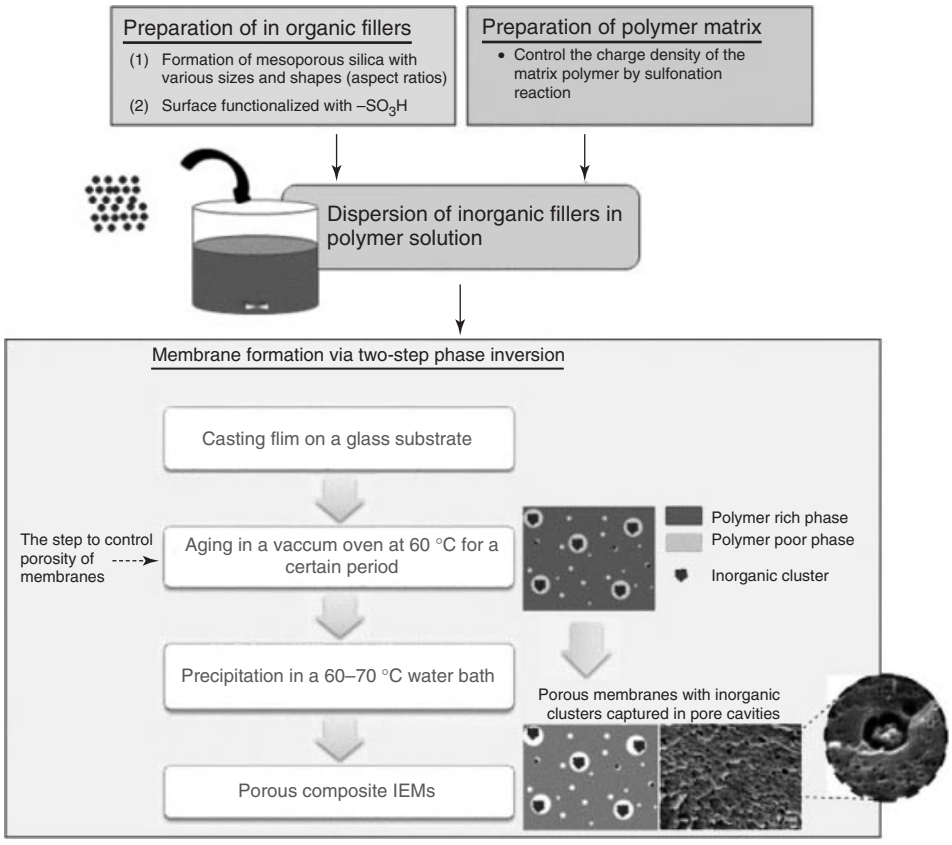

Figure 6.13 Preparation procedure of the composite IEMs via two-step phase inversion.

as the agglomerates interfere with the charged functional groups of the polymer matrix. Therefore, it is crucially important to optimize the loading to prepare membranes with overall good properties.

It is important to mention that the choices of preparation routes have to be wisely selected for a designed composite. Although good interaction between fillers and matrix give advantages for mechanical and thermal stability, it is normally at the cost of the reduction of functional groups for ion exchange and suppression of the membrane conductivity [106, 112, 113, 123, 126]. In many cases, the IEC and conductivities of the membranes decreased because of the incorporation of inorganic fillers, interfering with the functional groups of the polymer matrix [112, 113, 123, 126]. Therefore, optimization is of crucial importance and the percolation studies are recommended.

6.3.3
Membranes with Specific Properties

Although the properties and performance of the IEMs have been significantly improved over the last five decades, they are still insufficient for separating specific ionic species in some niche applications. Several strategies, including modifying membrane surface and their hydrophilicity, changing the structure and porosity of membranes, and incorporating special functional groups in polymer chains or fillers have been proposed .

In general, permselectivity among ions in a mixed solution through selective membranes depends on the affinity of the components with the membrane and the migration rate of each component in the membrane phase [128, 129].

Sieving monovalent ions such as NaCl from other multivalent ions has been studied mainly by modification of IEMs, making the membrane matrix dense or forming a thin dense layer on the surface. This is the simplest concept to change permselectivity of IEMs. One simple method to make membranes dense is to increase cross-linkage of the membranes, resulting in tunable pore sizes of the membranes and then adjustable selectivity between bulkier molecules and smaller molecules [134, 135]. However, the result appears to be not that simple. The transport number of ions depends not only on the size of ions but also on the Gibbs hydration energies of the ions. Although increasing cross-linkage enhances the permselectivity of the membrane, it also increases electrical resistance of the membrane. Therefore, conducting polymers were applied and a dense layer on the membrane surface is more preferable to avoid the increase of resistance. Figure 6.14 shows some chemical structures of conducting polymers.

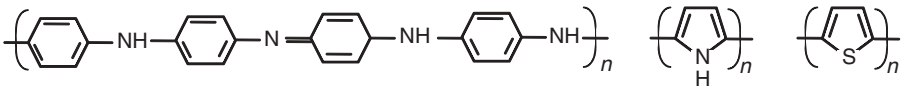

Figure 6.14 Structures of conducting polymers.

The conductive nature of conducting polymers is associated with unique conjugate bonds along the polymer backbones that allows electrons to freely transport through when an electrical potential is applied [138]. Polypyrrole is extremely rigid and has good affinity to IEMs [79, 136, 138]. It can easily form highly dense structure or tightly bonded layer on the membrane surface by impregnation of conducting polymers into the membrane matrix or ion exchange with the cation exchangeable groups on the membrane surface [137]. Moreover, polypyrrole possesses secondary amino groups, which affect the permselectivity between charged ions. It has been reported that the permselectivity of divalent ions compared to NaCl decreased because of the synergistic sieving effect of dense polypyrrole layer and the difference of repulsion forces among ions with the membranes [139]. For more examples of membrane surface modification by conducting polymer, polyaniline (PANI) has also been reported to affect the selectivity of monovalent ions from multivalent ions [138, 140–142]. It has been proposed that a reduction in transport number of divalent ions compared with monovalent ions through both composite PANI/AEMs and CEMs may be a result of three factors; the electrostatic repulsions increasing the difficulty for multivalent ions to pass through the membranes, the decrease of hydrophilicity of membranes resulting in the reduction of interaction with more hydrated ions, and the partial reduction or increment in the surface charge density of AEM/PANI and CEM/PANI.

The formation of a thin cationic charged layer on the surface of CEMs has been reported to be another effective method to separate monovalent ions from multivalent ions [128–130, 143, 144]. Cationic polyelectrolytes such as the amino groups of polyethyleneimine which adsorbed on IEMs without ion exchanging with sulfonic groups of the membranes are thought to be due to highly branched structure of polyethyleneimine. Therefore, most positive charges from the modifier and negative charges from the CEMs remain and the presence of these positive charges results in difficulties for multivalent ions to pass through the membranes owing to higher repulsion force.

Sata *et al*. has systematically investigated the influence of membrane hydrophilicity on the selectivity of anion species compared to chloride ions [17, 131, 132, 134, 135, 137]. It is apparent that the transport number of anions through AEMs was predominated by the hydration energy of anions rather than their hydrated size [128]. For instance, AEMs with increased hydrophilicity showed the significant decrease of transport number of fluoride ions, which are strongly hydrated anions compared to chloride ions. A similar trend was also observed in the case of sulfate ions. In contrast, for nitrate ions with similar hydrated ion size but less hydration energy compared to the chloride ions, the mobility ratio of the nitrate ions to chloride ions was increased with the decreased hydrophilicity of the AEM. Therefore, the understanding of the relationship between hydrophilicity of AEMs and hydration energy of anions is of great importance. It is expected that by decreasing hydrophilicity of the AEMs, less hydrated anions can permeate through the membranes more easily than strongly hydrated anions [17] (Table 6.4).

Ether compounds such as ethylene glycol, dipropylene glycol, and dimethyl ether have been used to change the hydrophilicity of IEMs in order to change

Table 6.4 Ionic radius, hydrate ionic radius, and hydration energy of ion species [158, 159].

Ion	Ionic radius (nm)	Hydrated ionic radius (nm)	Hydration energy (kJ mol^{-1})
Na^+	0.095	0.365	407
Mg^{2+}	0.074	0.429	1921
Ca^{2+}	0.099	0.349	1584
Cl^-	0.181	0.347	376
NO_3^-	0.189	0.340	270
SO_4^{2-}	0.230	0.380	1138

permselectivity of membranes. Owing to the existence of ether groups and alcoholic groups, these compounds possess a hydrophilic nature, which is expected to make stronger hydrated ions permeate through the membranes more easily than less hydrated ions [131–133]. However, because these compounds are soluble in water, it was found that glycol compounds were dissolved from the membranes during ED, which is undesirable.

6.3.3.1 Improving Antifouling Property

Fouling is one of the most serious problems for membrane separation processes including IEM ED. It decreases the performance efficiency of the membranes. It is well known that AEMs often suffer from fouling more than CEMs do, because many organic foulants in solution are in anionic forms and can therefore stick to the surface of AEMs. There are many techniques that have been proposed to prevent fouling of IEMs. These may be grouped into two main categories, by promoting foulants to permeate easily through the membranes and by prohibiting foulants to pass through IEMs.

The structures of membranes were loosened to allow organic macroions to easily permeate through as a method to facilitate the transmission of foulants [145]. However, there was an undesirable effect of the decrease of ion selectivity of IEMs by loosening the structure of the membranes.

On the other hand, to prevent foulants penetrating through membranes a dense structure or thin layer of positively charged group on the membrane surface was introduced. Unfortunately, as a consequence, the resistance of membranes increased dramatically.

Recently, new techniques to improve resistance against organic fouling without significant increase of electrical resistance of the membranes have been patented [146].

It has been proved that the fixation of polyether compounds on the surface or inside the membranes prevents ion exchange groups of the membranes from the direct contact with organic macroions, which prohibits the absorption of them. To avoid the ether compounds dissolving during ED, the compounds were fixed by decomposing the ether bond of polyether compounds with an ether bound cleavage

reagent such as a mixture of acetic anhydride-*p*-toluene sulfonic acid, phosphoric acid, and hydrobromic acid. The results demonstrated excellent fouling resistance and low electrical resistance (1.5–3.4 Ω cm^{-2}) in the membranes.

The surface property of membranes is one of the most important factors affecting organic fouling in membrane separation processes. It has been reported that the colloid and microbial foulants favor the adsorption on hydrophobic surface [147, 148]. Thus, the hydrophilic modification of the membrane surface becomes a potential method to prevent fouling. TiO_2/polymer self-assembly method has been used to modify hydrophilicity of polymeric membranes to decrease the fouling rate [147, 148]. This method is based on the ionic attraction between the oppositely charged species of TiO_2 particles and membranes, which promotes the adhesion between them [147–149]. The result showed that organic fouling in membranes modified with TiO_2 nanoparticles decreased compared with the unmodified one because of the increase of hydrophilicity of the membrane. Moreover, the adsorbed foulants on the tested membranes were more easily removed by shear force than those on unmodified membranes.

6.4 Future Perspectives of IEMs

The first industrial application of IEMs was in the field of desalination by ED. The recent development of fundamental theory has led to expanded applications to various fields such as electrodialysis reversal (EDR), electrodeionization (EDI), bipolar-membrane electrodialysis (BMED), and fuel cell [2]. In this section, the recently developed IEMs and their perspectives particularly relevant to ED process, water purification, and desalination fields are highlighted.

Although desalination is an important technology that offers a solution for the world water crisis, the energy consumption, and production cost of this technology remains a great challenge.

Tremendous efforts have been dedicated to reduce the energy consumption of desalination technology and to bring down the water production cost to affordable levels. Besides the development of novel membranes, new process designs for operating systems that can work more effective are increasingly concerned [150, 151].

6.4.1 Hybrid System

Another strategy for reducing the overall cost of desalination is the use of hybrid system, a system that combines two or more desalination processes [84, 150, 152, 153]. The hybrid desalination system has recently gained intensive attention as it can offer a better separation performance for specific industrial separation and a process with optimized utilization of material and energy [84, 150, 152]. Electro-driven processes such as ED has been integrated with pressure-driven membrane

operation such as microfiltration (MF), ultrafiltration (UF), nanofiltration (NF), and reverse osmosis (RO). Such hybrid systems showed better performance in water treatment and desalination compared to their conventional process [5–7, 154, 155]. Recently, a novel RO–ED hybrid system was proposed by Pellegrino *et al.* [5] that aimed to reduce the osmotic pressure at the interface of RO membrane, to reduce the energy consumption, and to improve the water recovery of the system. Their design is shown in Figure 6.15; the hollow-fiber RO membranes were packed in ED compartments between CEM and AEM. The stack of the hollow-fiber RO

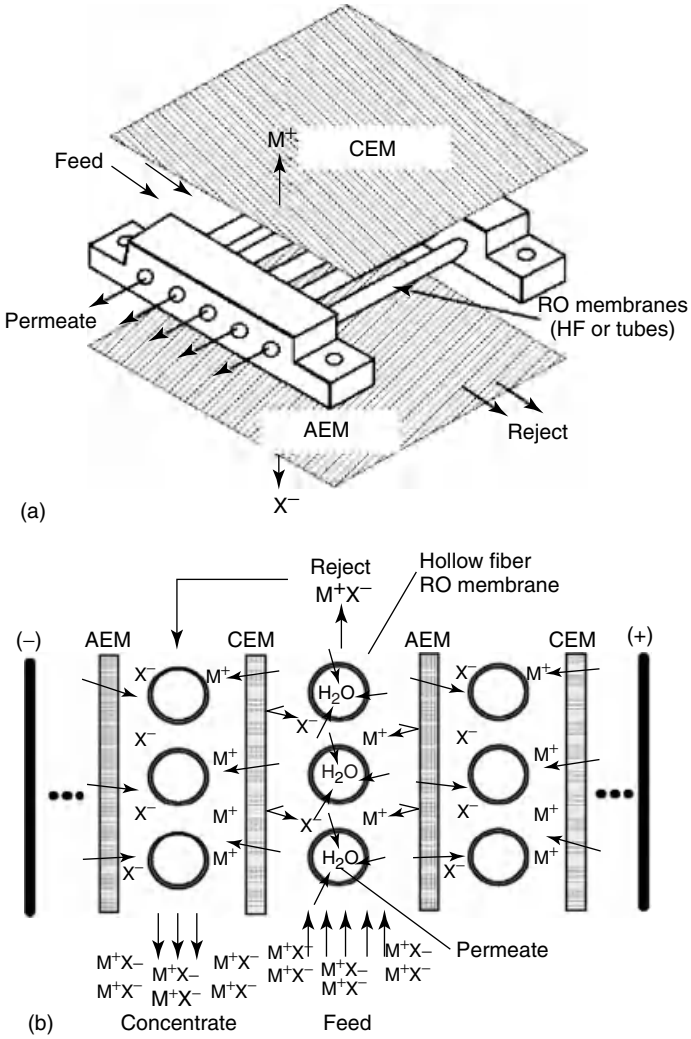

Figure 6.15 Schematic (a) cell pair in the hybrid RO-ED system and (b) stack configuration for the hybrid RO–ED. The M^+ and X^- represents cations and anions, respectively [5].

membranes may be considered to act as the spacer in the conventional ED system that helps the well mixing of the feed solution and promotes the turbulent flow of the system. This in turn suppresses the concentration polarization effects near the membrane interface. Their initial analysis of this new hybrid system design under different operating conditions indicated that the energy saving of 10–20% can be obtained.

However, the modeling analysis from this work also indicated the limiting factor of the conductivity of the IEMs on the energy consumption of the system. Therefore, the robust membranes are vital to be further developed for supporting the use of such a novel conceptual system design.

6.4.2
Small-Scale Seawater Desalination

Capital- and energy-intensive desalination plants that require seawater conveyance and reliable power supply for the system are still impractical and uneconomical at small scale for personal use or small villages in a remote area. Recently, research groups in Massachusetts Institute of Technology and Pohang University of Science and Technology have designed a novel small seawater desalination unit, the so-called ion-concentration polarization (ICP) desalination system (Figure 6.16) with the possibility of battery-powered operation [157, 156]. New system for small-scale desalination by ICP, is considered as the latest state-of-the-art system capable of continuous seawater desalination with high salt rejection of 99% at low power consumption of less than 3.5 Wh l^{-1} [156].

This work represents another example of novel conceptual nanoscale design based on theoretical study that have been proved by experimental implementation to be an excellent tool for providing fresh water for personal use in remote areas. Again, porous IEMs suitable to be used in such an innovative concept have to be further developed.

6.5
Conclusions

The present overview on the development of IEMs has addressed the vital role of IEMs involved in desalination and water purification applications. The properties and separation capabilities determine the performance of membranes. In the past decades, interdisciplinary approaches have been applied to the development of new IEMs. IEMs can be designed and prepared by a number of strategies varying from basic polymer reactions to advanced nanotechnology via molecular design and architectural tailoring of composite materials. However, to satisfy the membrane requirements for specific applications, the targeted properties of IEMs have to be set up, and appropriate synthesis routes for IEMs toward the targets should be specified accordingly. To accomplish this, fundamental understanding of the relationship among preparation conditions, structures, and functions of the IEMs

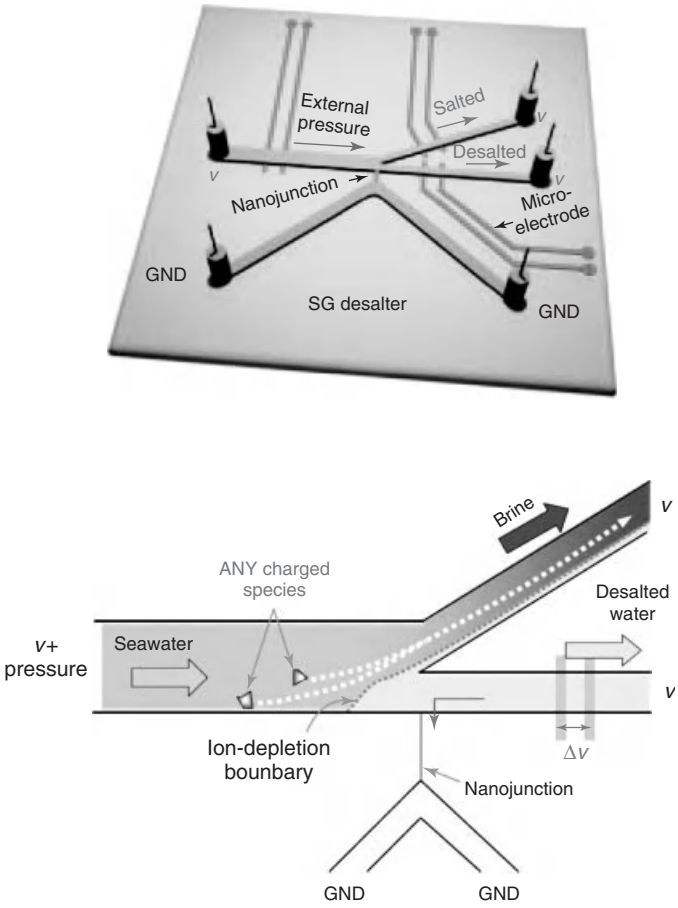

Figure 6.16 ICP desalination scheme: (a) micro/nanofluidic desalination system with embedded microelectrode for the measuring potential drop and (b) electrokinetic desalination operation associated with the external pressure [156].

have to be established. Furthermore, more efforts and attention should be paid to the following studies:

- percolation study of the membrane preparation, structure, and properties;
- elucidation of transport phenomena of newly prepared membranes, as well as the search for their new application;
- evaluation of new membranes in an application;
- the study of surface chemistry and architecture of membranes to reduce the effects of concentration polarization; and
- the modification of surface chemistry toward high fouling resistance properties of IEMs.

From the viewpoint of material engineering, nanotechnology offers powerful tools to tailor and develop novel membranes. Among several approaches presented in this chapter, the concept of composite design stands out as an interesting strategy for developing IEMs. The properties of membranes can be designed via the selection of component materials and the tailoring of desired functionalities to each component. Encouragingly, the preparation procedure of composite membranes is relatively simple, and thus, has a high potential for large-scale commercialization. Although this concept has drawn much attention in fuel cell application, the utilization of this strategy in the development of IEMs for desalination is still very limited, leaving us much room for development and comprehensive study of composite design and their applications in desalination.

Apart from the material development, the system design and their operation optimization should also be further developed. In the desalination application which is one of the major practical areas for the IEMs, new systems to bring down the energy consumption and production cost require more progress in comparison to more widely used processes such as RO. Such system designs that can combine with renewable energy sources or can work more effectively should also be emphasized for the sustainable development of energy-saving and environment friendly systems.

References

1. Schoeman, J.J., Steyn, A., and Makgae, M. (2005) Evaluation of electrodialysis for the treatment of an industrial solid waste leachate. *Desalination*, **186**, 273–289.
2. Koter, S. and Warszawski, A. (2000) Electromembrane processes in environment protection. *Pol. J. Environ. Stud.*, **9**, 45–56.
3. Ortiz, J.M. *et al.*, (2006) Photovoltaic electrodialysis system for brackish water desalination: Modeling of global process. *J. Membr. Sci.*, **274**, 138–149.
4. Ortiz, J.M. *et al.*, (2005) Brackish water desalination by electrodialysis; batch recirculation operation modeling. *J. Membr. Sci.*, **252**, 65–75.
5. Pellegrino, J., Gorman, C., and Richards, L. (2007) A speculative hybrid reverse osmosis/electrodialysis unit operation. *Desalination*, **214**, 11–30.
6. Turek, M. and Dydo, P. (2008) Comprehensive utilization of brackish water in ED-thermal system. *Desalination*, **221**, 455–461.
7. Xu, T. and Huang, C. (2008) Electrodialysis-based separation technologies: a critical review. *Am. Inst. Chem. Eng.*, **54**, 3147–3159.
8. Luo, Q. *et al.*, (2008) Preparation and characterization of Nafion/SPEEK layered composite membrane and its application in vandium redox flow battery. *J. Membr. Sci.*, **325**, p. 553–558.
9. Hansen, H.K., O.L.M., and Villumsen, A. (1999) Electrical resistance and transport numbers of ion-exchange membranes used in electrodialytic soil remediation. *Sep. Sci. Technol.*, **34**, p. 2223–2233.
10. Smalley, R.E. (2005) Future global energy prosperity: The terawat challenge. *MRS Bull.*, **30**, p. 412–417.
11. Strathmann, H., (2004) *Ion-Exchange Membrane Separation Processes*, Membrane Science and Technology Series, Vol. 9, Elsevier, Amsterdam and Boston, xi, 348 p.
12. Dzyazko, Y.S. and Belyakov, V.N. (2004) Purification of a diluted nickel solution

containing nickel by a process combining ion exchange and electrodialysis. *Desalination*, **162**, 179–189.
13. Sadrzadeh, M. *et al.*, (2008) Separation of lead ions from wastewater using electrodialysis: Comparing mathematical and neural network modeling. *Chem. Eng. J.*, **144**, 431–441.
14. Balster, J., Stamatialis, D.F., and Wessling, M. (2004) Electro-catalytic membrane reactors and the development of bipolar membrane technology. *Chem. Eng. Process.*, **43**, 1115–1127.
15. Tsang, E.M.W. *et al.*, (2009) Nanostructure, morphology and properties of fluorous copolymers bearing ionic grafts. *Macromolecules*, **42**, 9467–9480.
16. Qiu, J. *et al.*, (2009) Performance of vanadium redox flow battery with a novel amphoteric ion exchange membrane synthesized by two-step grafting method. *J. Membr. Sci.*, **324**, 215–220.
17. Sata, T. (2002) *Ion Exchange Membranes. Preparation, Characterization, Modification and Application*, The Royal Society of Chemistry, Cambridge.
18. Nagarale, R.K., Gohil, G.S., and Shahi, V.K. (2006) Recent developments on ion-exchange membranes and electromembrane processes. *Adv. Colloid Interface Sci.*, **119** (2–3), 97–130.
19. Division, National Chemical Research Laboratory Process Development (1960) *Demineralization by Electrodialysis*, Butterworths Scientific, London.
20. Lakshminarayanaiah, N. (1969) *Transport Phenomena in Membranes*, Academic Press, Inc., New York.
21. Wilson, J.R. (1960) *Demineralization by Electrodialysis*, The University Press, Glasgow, London.
22. Mulder, M. (1991) *Basic Principles of Membrane Technology*, Kluwer Academic Publishers, Dordrecht.
23. Nikonenko, V.V. *et al.*, (2010) Intensive current transfer in membrane systems; Modelling, mechanisms and application in electrodialysis. *Adv. Colloid. Interface Sci.*, **160**, 101–123.
24. Baker, R.W. (2004) *Membrane Technology and Applications*, John Wiley & Sons, Ltd.
25. Tanaka, Y. (2007) Ion exchange membrane-Fundamentals and applications. *J. Membr. Sci.*, **12**, 139–186.
26. Lakshminarayanaiah, N. (1965) Transport phenomena in artificial membranes. *Chem. Rev.*, **65**, 491–565.
27. Balster, J. *et al.*, (2007) Morphology and microtopology of cation-exchange polymers and the origin of the overlimiting current. *J. Phys. Chem.*, **111**, 2152–2165.
28. Zabolotsky, V.I. *et al.*, (1998) Coupled transport phenomena in overlimiting current electrodialysis. *Sep. Purif. Technol.*, **14**, 255–267.
29. Tanaka, Y. and Seno, M. (1986) Concentration polarization and water dissociation in ion-exchange membrane electrodialysis. *J. Chem. Soc., Faraday Trans.*, **82** (1), 2065–2077.
30. Krol, J.J., Wessling, H., and Strathmann, H. (1999) Chronopotentiometry and overlimiting ion transport through monopolar ion exchange membranes. *J. Membr. Sci.*, **162**, 155–164.
31. Krol, J.J., Wessling, H., and Strathmann, H. (1999) Concentration polarization with monopolar ion exchange membranes: current–voltage curves and water dissociation. *J. Membr. Sci.*, **162**, 145–154.
32. Lee, H.-J. *et al.*, (2008) Influence of the heterogeneous structure on the electrochemical properties of anion exchange membranes. *J. Membr. Sci.*, **320**, 549–555.
33. Block, M. and Kitchener, J.A. (1966) Polarization phenomena in commercial ion-exchange membranes. *J. Electrochem. Soc.*, **113** (9), 947–953.
34. Tanaka, Y. (2004) Concentration polarization in ion-exchange membrane electrodialysis: The events arising in an unforced flowing solution in a desalting cell. *J. Membr. Sci.*, **244** (1–2), 1–16.
35. Pismenskaia, N.D. *et al.*, (2007) Coupled convection of solution near the surface of ion-exchange membranes in intensive current regimes. *Russ. J. Electrochem.*, **43**, 325–345.
36. Patel, R.D. and Lang, K.-C. (1977) Polarization in ion-exchange membrane electrodialysis. *Ind. Eng. Chem. Fundam.*, **16**, 340–348.

37. Aguilella, V.M. *et al.*, (1991) Current–voltage curves for ion-exchange membranes. Contributions to the total potential drop. *J. Membr. Sci.*, **61**, 177–190.
38. Ray, P. *et al.*, (1999) Transport phenomenon as a function of counter and co-ions in solution: chronopotentiometric behavior of anion exchange membrane in different aqueous electrolyte solutions. *J. Membr. Sci.*, **160**, 243–254.
39. Choi, J.-H., Park, J.-S., and Moon, S.-H. (2002) Direct measurement of concentration distribution within the boundary layer of an ion-exchange membrane. *J. Colloid Interface Sci.*, **251**, 311–317.
40. Pismenskaya, N. *et al.*, (2004) Chronopotentiometry applied to the study of ion transfer through anion exchange membranes. *J. Membr. Sci.*, **228**, 65–76.
41. Rubinshtein, I. *et al.*, (2002) Experimental verification of the electroosmotic mechanism of overlimiting conductance through a cation exchange electrodialysis membrane. *Russ. J. Electrochem.*, **38**, 853–863.
42. Metayer, M., Bourdillon, C., and Selegny, E. (1973) Concentration polarization on ion-exchange membranes in electrodialysis with natural convection. *Desalination*, **13**, 129–146.
43. Larchet, C. *et al.*, (2008) Application of chronopoteniometry to determine the thickness of diffusion layer adjacent to an ion-exchange membrane under natural convection. *Adv. Colloid. Interface Sci.*, **139**, 45–61.
44. Loza, N.V. *et al.*, (2006) Effect of modification of ion-exchange membrane MF-4SK on its polarization characteristics. *Russ. J. Electrochem.*, **42** (8), 815–822.
45. Elattar, A. *et al.*, (1998) Comparison of transport properties of monovalent anions through anion-exchange membranes. *J. Membr. Sci.*, **143** (1–2), 249–261.
46. Volodin, E. *et al.*, (2005) Ion transfer across ion-exchange membranes with homogeneous and heterogeneous surfaces. *J. Colloid Interface Sci.*, **285**, 247–258.
47. Vyas, P.V. *et al.*, (2003) Studies of the effect of variation of blend ratio on permselectivity and heterogeneity of ion-exchange membranes. *J. Colloid Interface Sci.*, **257**, 127–134.
48. Wilhelm, F.G. *et al.*, (2001) Chronopotentiometry for the advanced current–voltage characterisation of bipolar membranes. *J. Electroanal. Chem.*, **502**, 152–166.
49. Choi, J.-H., Lee, H.-J., and Moon, S.-H. (2001) Effects of electrolytes on the transport phenomena in a cation-exchange membrane. *J. Colloid Interface Sci.*, **238**, 188–195.
50. Meng, H. *et al.*, (2005) A new method to determine the optimal operating current (I_{lim}') in the electrodialysis process. *Desalination*, **181**, 101–108.
51. Pismenskaia, N. *et al.*, (2004) Chronopotentiometry applied to the study of ion transfer through anion exchange membranes. *J. Membr. Sci.*, **228**, 65–76.
52. Ibanez, R., Stamatialis, D.F., and Wessling, M. (2004) Role of membrane surface in concentration polarization at cation-exchange membranes. *J. Membr. Sci.*, **239**, 119–128.
53. *http://www.fumatech.com/Startseite/Produkte/fumasep/Ionenaustauscher-membranen/* (accessed 1 March 2008).
54. Lee, H.-J. *et al.*, (2002) Designing of an electrodialysis desalination plant. *Desalination*, **142**, 267–286.
55. Feng, S. *et al.*, (2009) Synthesis and characterization of crosslinked sulfonated poly(arylene ether sulfone) membranes for DMFC applications. *J. Membr. Sci.*, **335**, 13–20.
56. Iojoiu, C. *et al.*, (2005) Mastering sulfonation of aromatic polysulfones: Crucial for membranes for fuel cell application. *Fuel Cells*, **5** (3), 344–354.
57. Johnson, B.C. *et al.*, (1984) Synthesis and characterization of sulfonated poly(arylene ether sulfones). *J. Polym. Sci. Polym. Chem. Ed.*, **22**, 721–737.
58. Klaysom, C. *et al.*, (2010) Synthesis and characterization of sulfonated polyethersulfone for cation-exchange membranes. *J. Membr. Sci.*, **368**, 48–53.
59. Roziere, J. and Jones, D.J. (2003) Non-fluorinated polymer materials for

proton exchange membrane fuel cells. *Annu. Rev. Mater. Res.*, **33**, 503–555.
60. Dai, H. *et al.*, (2007) Development and characterization of sulfonated poly(ether sulfone) for proton exchange membrane materials. *Solid State Ion.*, **178**, 339–345.
61. Nagarale, R.K. *et al.*, (2005) Preparation and electrochemical characterization of sulfonated polysulfone cation-exchange membranes: Effects of the solvents on the degree of sulfonation. *J. Appl. Polym. Sci.*, **96**, 2344–2345.
62. Li, Y. and Chung, T.-S. (2008) Highly selective sulfonated polyethersulfone (sPES)-based membranes with transition metal counterions for hydrogen recovery and natural gas separation. *J. Membr. Sci.*, **308**, 128–135.
63. Guan, R. *et al.*, (2005) Polyethersulfone sulfonated by chlorosulfonic acid and its membrane characteristics. *Eur. Polym. J.*, **41**, 1554–1560.
64. Klaysom, C. *et al.*, (2011) Preparation of porous ion-exchange membranes (IEMs) and their applications. *J. Membr. Sci.*, **371**, 37–44.
65. Kerres, J., W.C., and Reichle, S. (1996) New sulfonated engineering polymers via the metalation route. I. Sulfonated poly(ethersulfone) PSU Udel via metalation-sulfination-oxidation. *J. Polym. Sci., Part A: Polym. Chem.*, **34**, 2421–2438.
66. Kerres, J. *et al.*, (1998) Development and characterization of crosslinked ionomer membranes based upon sulfinated and sulfonated PSU crosslinked PSU blend membranes by disproportionation of sulfinic acid groups. *J. Membr. Sci.*, **139**, 211–225.
67. Byun, I.S., Kim, I.C., and Seo, J.W. (2000) Pervaporation behavior of asymmetric sulfonated polysulfones and sulfonated poly(ether sulfone) membranes. *J. Appl. Polym. Sci.*, **76**, 787–798.
68. Noshay, A. and Robeson, L.M. (1976) Sulfonated polysulfone. *J. Appl. Polym. Sci.*, **20**, 1885–1903.
69. Li, L. and Wang, Y. (2005) Quaternized polyethersulfone Cardo anion exchange membrane for direct methanol alkaline fuel cells. *J. Membr. Sci.*, **262**, 1–4.
70. Evram, E. *et al.*, (1997) Polymers with pendant functional group. III. Polysulfones containing viologen group. *J. Macromol. Sci., A Pure Appl. Chem.*, **34**, 1701–1714.
71. Bailly, C. *et al.*, (1987) The sodium salts of sulphonated poly(aryl-ether-ether-ketone)(PEEK): preparation and characterization. *Polymer*, **28**, 1009–1016.
72. Jin, X. *et al.*, (1985) A sulphonated poly(aryly ether ketone). *Br. Polym. J.*, **17**, 4–10.
73. Kobayashi, T. *et al.*, (1998) Protn-conducting polymers derived from poly(ether-etherketone) and poly(4-phenoxybenzoyl-1,4-phenylene). *Solid State Ion.*, **106**, 219–225.
74. Zaidi, S.M.J. *et al.*, (2000) Proton conducting composite membranes from polyether ether ketone and heteropolyacids for fuel cell applications. *J. Membr. Sci.*, **173**, 17–34.
75. Do, K.N.T. and Kim, D. (2008) Synthesis and characterization of homogeneously sulfonated poly(ether ether ketone) membranes: Effect of casting solvent. *J. Appl. Polym. Sci.*, **40**, 1763–1770.
76. Fang, J. and Shen, P.K. (2006) Quaternized poly(phthalazinon ether sulfone ketone) membrane for anion exchange membrane fuel cells. *J. Membr. Sci.*, **285**, 317–322.
77. Trotta, F. *et al.*, (1998) Sulfonation of polyetheretehrketone by chlorosulfuric acid. *J. Appl. Polym. Sci.*, **70**, 478–483.
78. Drioli, E. *et al.*, (2004) Sulfonated PEEK-WC membranes for possible fuel cell applications. *J. Membr. Sci.*, **228**, 139–148.
79. Cui, W., Kerres, J., and Eigenberger, G. (1998) Development and characterization of ion-exchange polymer blend membranes. *Sep. Purif. Technol.*, **14**, 145–154.
80. Tongwen, X. and Weihua, Y. (2001) Fundamental studies of a new series of anion exchange membranes: membrane preparation and characterization. *J. Membr. Sci.*, **190**, 159–166.
81. Wu, C. *et al.*, (2005) Synthesis and characterizations of new negatively charged organic–inorganic hybrid materials,

Part II. Membrane preparation and characterizations. *J. Membr. Sci.*, **247**, 111–118.

82. Xu, C., Xu, T., and Yang, W. (2003) A new inorganic–organic negatively charged membrane: membrane preparation and characterization. *J. Membr. Sci.*, **224**, 117–125.

83. Tongwen, X. and Zha, F.F. (2002) Fundamental studies on a new series of anion exchange membrane: Effect of simultaneous amination-crosslinking processes on membranes ion-exchange capacity and dimensional stability. *J. Membr. Sci.*, **199**, 203–210.

84. Xu, T. (2005) Ion exchange membranes: state of their development and perspective. *J. Membr. Sci.*, **263**, 1–29.

85. Kang, M.-S. *et al.*, (2003) Electrochemical characterization of sulfonated poly(arylene ether sulfone) (S-PES) cation-exchange membranes. *J. Membr. Sci.*, **216** (1–2), 39–53.

86. Krishnan, N.N. *et al.*, (2006) Synthesis and characterization of sulfonated poly(ether sulfone) copolymer membranes for fuel cell applications. *J. Power Sources*, **158**, 1246–1250.

87. Sankir, M. *et al.*, (2006) Synthesis and characterization of 3,3′-disulfonated-4,4′-dichlorodiphenyl sulfone (SDCDPS) monomer for proton exchange membranes (PEM) in fuel cell application. *J. Appl. Polym. Sci.*, **100**, 4595–4602.

88. Ueda, M. *et al.*, (1993) Synthesis and characterization of aromatic poly(ether sulfone)s containing pendant sodium sulfonate groups. *J. Polym. Sci., A Polym. Chem.*, **31**, 853–858.

89. Kim, Y.S. *et al.*, (2004) Sulfonated poly(arylene ether sulfone) copolymer proton exchange membranes: composition and morphology effects on the methanol permeability. *J. Membr. Sci.*, **243**, 317–326.

90. Wang, F. *et al.*, (2001) Synthesis of highly sulfonated poly(arylene ether sulfone) random (statistical) copolymers via direct polymerization. *Marcomol. Symp.*, **175**, 387–395.

91. Kato, K. *et al.*, (2003) Polymer surface with graft chains. *Prog. Polym. Sci.*, **28**, 209–259.

92. Choi, S.-H., Lee, K.-P., and Nho, Y.C. (1999) Electrochemical properties of polyethylene membrane modified with sulfonic acid group. *Korea Polym. J.*, **7**, 297–303.

93. Nasef, M.M. and Saidi, H. (2005) Structure–property relationships in radiation grafted poly(tetrafluoroethylene)-graft-polystyrene sulfonic acid membranes. *J. Polym. Res.*, **12**, 305–312.

94. Sunaga, K. *et al.*, (1999) Characteristics of porous anion-exchange membranes prepared by cografting of glycidyl methacrylate with divinylbenzene. *Chem. Mater.*, **11**, 1986–1989.

95. Lee, K.-P., Choi, S.-H., and Kang, H.-D. (2002) Preparation and characterization of polyalkene membranes modified with four different ion-exchange groups by radiation-induced graft polymerization. *J. Chromatogr. A*, **948**, 129–138.

96. Gupta, B. and Chapiro, A. (1989) Preparation of ion-exchange membranes by grafting acrylic acid into pre-irradiated polymer films-1. grafting into polyethylene. *Eur. Polym. J.*, **25**, 1137–1143.

97. Yamee, B. *et al.*, (2010) Hybrid polymer-silicon proton conducting membranes via a pore-filling surface-initiated polymerization approach. *Appl. Mater. Interfaces*, **2**, 279–287.

98. Gupta, B. and Chapiro, A. (1989) Preparation of ion-exchange membranes by grafting acrylic acid into pre-irradiated polymer films – 2.Grafting into teflon-FEP. *Eur. Polym. J.*, **25**, 1145–1148.

99. Gubler, L. *et al.*, (2009) Radiation grafted fuel cell membranes based on co-grafting of alpha-methylstyrene and methacrylonitrile into a fluoropolymer base film. *J. Membr. Sci.*, **339**, 68–77.

100. Gupta, B., Buchi, F.N., and Scherer, G.G. (1994) Cation exchange membranes by pre-irradiation grafting of styrene into FEP films. I. Influence of synthesis conditions. *J. Polym. Sci., A Polym. Chem.*, **32**, 1931–1938.

101. Gupta, B. *et al.*, (1996) Crosslinked ion exchange membranes by radiation grafting of styrene/divinylbenzene into FEP films. *J. Membr. Sci.*, **118**, 213–238.

102. Nasef, M.M., Saidi, H., and Nor, H.M. (2000) Cation exchange membranes

by radiation-induced graft copolymerization of styrene onto PFA copolymer films. III. Thermal stability of the membranes. *J. Appl. Polym. Sci.*, **77**, 1877–1885.

103. Danks, T.N., Slade, R.C.T., and Varcoe, J.R. (2003) Alkaline anion-exchange radiation-grafted membranes for possible electrochemical application in fuel cell. *J. Mater. Chem.*, **13**, 712–721.

104. Herman, H., Slade, R.C.T., and Varcoe, J.R. (2003) The radiation-grafting of vinylbenzyl chloride onto poly(hexafluoropropylene-co-tetrafluoroethylene) films with subsequent conversion to alkaline anion-exchange membranes: optimisation of the experimental conditions and characterisation. *J. Membr. Sci.*, **218**, 147–163.

105. Nasef, M.M. and Hegazy, E.-S.A. (2004) Preparation and applications of ion exchange membranes by radiation-induced graft copolymerization of polarmonomers onto non-polar films. *Prog. Polym. Sci.*, **29**, 449–561.

106. Lavorgna, M. *et al.*, (2007) Hybridization of Nafion membranes by the infusion of functionalized siloxane precursors. *J. Membr. Sci.*, **294**, 159–168.

107. Oh, S.-Y. *et al.*, (2010) Inorganic–organic composite electrolytes consisting of polybenzimidazole and Cs-substituted heteropoly acids and their application for medium temperature fuel cells. *J. Mater. Chem.*, **20**, 6359–6366.

108. Mauritz, K.A. *et al.*, (2004) Self-assembled organic/inorganic hybrids as membrane materials. *Electrochim. Acta*, **50**, 565–569.

109. Zou, J., Zhao, Y., and Shi, W. (2004) Preparation and properties of proton conducting organic–inorganic hybrid membranes based on hyperbranched aliphatic polyester and phosphoric acid. *J. Membr. Sci.*, **245**, 35–40.

110. Duvdevani, T. *et al.*, (2006) Novel composite proton-exchange membrane based on silica-anchored sulfonic acid (SASA). *J. Power Sources*, **161**, 1069–1075.

111. Wu, C., Xu, T., and Yang, W. (2005) Synthesis and characterizations of novel, positively charged poly(methyl acrylate)–SiO2 nanocomposites. *J. Membr. Sci.*, **41**, 1901–1908.

112. Li, C. *et al.*, (2006) Casting Nafion-sulfonated organosilica nano-composite membranes used in direct methanol fuel cells. *J. Membr. Sci.*, **272**, 50–57.

113. Chen, W.-F. and Kuo, P.-L. (2007) Covalently cross-linked perfluorosulfonated membranes with polysiloxane framework. *Macromolecules*, **40**, 1987–1994.

114. Ladewig, B.P. *et al.*, (2007) Nafion-MPMDMS nanocomposite membranes with low methanol permeability. *Electrochem. Commun.*, **9**, 781–786.

115. Lin, Y.-F. *et al.*, (2007) High proton-conducting Nafion/-SiO_3H functionalized mesoporous silica composite membranes. *J. Power. Sources*, **171**, 388–395.

116. Shahi, V.K. (2007) Highly charged proton-exchange membrane: Sulfonated poly(ether sulfone)-silica polyelectrolyte composite membranes for fuel cells. *Solid State Ion.*, **117**, 3395–3404.

117. Klaysom, C. *et al.*, (2011) Preparation of porous composite ion-exchange membranes for desalination application. *J. Mater. Chem.*, **21**, 7401–7409.

118. Klaysom, C. *et al.*, (2011) The influence of the particle size of surface functionalized additives on composite ion-exchange membranes. *J. Phys. Chem. C*, **115**, 15124–15132.

119. Klaysom, C. *et al.*, (2011) The effects of aspect ratio of inorganic fillers on structure, property, and performance of composite ion-exchange membranes. *J. Colloid Interface Sci.*, **363**, 431–439.

120. Marschall, R. *et al.*, (2012) Composite proton conducting polymer membranes for clean hydrogen production with solar light in a simple photoelectrochemical compartment cell. *Int. J. Hydrogen Energy*, **37**, 4012–4017.

121. Klaysom, C. *et al.*, (2010) Synthesis of composite ion-exchange membranes and their electrochemical properties for desalination applications. *J. Mater. Chem.*, **20**, 4669–4674.

122. Helen, M., Viswanathan, B., and Srinivasa Murthy, S. (2006) Fabrication and properties of hybrid membranes

based on salts of heteropolyacid, zirconium phosphate and polyvinyl alcohol. *J. Power Sources*, **163**, 433–439.

123. Fu, R.-Q., Hong, L., and Lee, J.Y. (2007) Membrane design for direct ethanol fuel cells: a hybrid proton-conducting interpenetrating polymer network. *Fuel Cells*, **1**, 52–61.

124. Nagarale, R.K. *et al.*, (2005) Preparation of organic–inorganic composite anion-exchange membranes via aqueous dispersion polymerization and their characterization. *J. Colloid Interface Sci.*, **287**, 198–206.

125. Binsu, V.V., Nagarale, R.K., and Shahi, V.K. (2005) Phosphonic acid functionalized aminopropyl triethoxysilane-PVA composite material: organic–inorganic hybrid proton-exchange membranes in aqueous media. *J. Mater. Chem.*, **15**, 4823–4831.

126. Nunes, S.P. *et al.*, (2002) Inorganic modification of proton conductive polymer membranes for direct methanol fuel cells. *J. Membr. Sci.*, **203**, 215–225.

127. Kickelbrick, G. (2003) Concepts for the incorporation of inorganic building blocks into organic polymers on a nanoscale. *Prog. Polym. Sci.*, **28**, 83–114.

128. Sata, T. (2000) Studies on anion exchange membranes having permselectivity for specific anions in electrodialysis-effect of hydrophilicity of anion exchange membranes on permselectivity of anions. *J. Membr. Sci.*, **167**, 1–31.

129. Sata, T., Sata, T., and Yang, W. (2002) Studies on cation-exchange membranes having permselectivity between cations in electrodialysis. *J. Membr. Sci.*, **206**, 31–60.

130. Sata, T. and Izuo, R. (1978) Modification of properties of ion exchange membranes V. Structure of cationic polyelectrolyte on the surface of cation exchange membranes. *Colloid Polym. Sci.*, **256**, 757–769.

131. Sata, T., Mine, K., and Matsusaki, K. (1998) Change in transport properties of anion-exchange membranes in the presence of ethylene glycols in electrodialysis. *J. Colloid Interface Sci.*, **202**, 348–358.

132. Sata, T. *et al.*, (1998) Changing permselectivity between halogen ions through anion exchange membranes in electrodialysis by controlling hydrophilicity of the membranes. *Faraday Trans.*, **94** (1), 147–153.

133. Sata, T. *et al.*, (1999) Transport properties of cation exchange membranes in the presence of ether compounds in electrodialysis. *J. Colloid Interface Sci.*, **219**, 310–319.

134. Sata, T., Teshima, K., and Yamaguchi, T. (1996) Permselectivity between two anions in anion exchange membranes crosslinked with various diamines in electrodialysis. *J. Polym. Sci., A Polym. Chem.*, **34** (8), 1475–1482.

135. Sata, T. and Nojima, S. (1999) Transport properties of anion exchange membranes prepared by the reaction of crosslinked membranes having chloromethyl groups with 4-vinylpyridine and trimethylamine. *J. Polym. Sci., B Polym. Phys.*, **37**, 1773–1785.

136. Sata, T. (1991) Properties of ion-exchange membranes combined anisotropically with conducting polymers. 2. Relationship of electrical potential generation to preparation conditions of composite membranes. *Chem. Mater.*, **3** (5), 838–843.

137. Sata, T., Yamaguchi, T., and Matsusaki, K. (1996) Preparation and properties of composite membranes composed of anion-exchange membranes and polypyrrole. *J. Phys. Chem.*, **100** (41), 16633–16640.

138. Pellegrino, J. (2003) The use of conducting polymers in membrane-based separations. *Ann. N. Y. Acad. Sci.*, **984**, 289–305.

139. Gohil, G.S., Binsu, V.V., and Shahi, V.K. (2006) Preparation and characterization of mono-valent ion selective polypyrrole composite ion-exchange membranes. *J. Membr. Sci.*, **280**, 210–218.

140. Nagarale, R.K. *et al.*, (2004) Preparation and electrochemical characterization of cation- and anion-exchange/polyaniline composite membrane. *J. Colloid Interface Sci.*, **277**, 162–171.

141. Amado, F.D.R. *et al.*, (2004) Synthesis and characterisation of high impact polystyrene/polyaniline composite membranes for electrodialysis. *J. Membr. Sci.*, **234**, 139–145.

142. Sata, T. *et al.*, (1999) Composite membranes prepared from cation exchange membranes and polyaniline and their transport properties in electrodialysis. *J. Electrochem. Soc.*, **146** (2), 585–591.

143. Stair, J.L., Harries, J.J., and Bruening, M.L. (2001) Enhancement of the ion-transport selectivity of layered polyelectrolyte membranes through cross-linking and hybridization. *Chem. Mater.*, **13**, 2641–2648.

144. Sata, T. and Mizutani, Y. (1979) Modification of properties of ion exchange membranes. VI Electrodialytic transport properties of cation exchange membranes with a electrodeposition layer of cationic polyelectrolytes. *J. Polym. Sci., Polym. Chem. Ed.*, **17**, 1199–1213.

145. Hodgdon, R.B., E.W., and Alexander, S.S. (1973) Macroreticular anion exchange membranes for electrodialysis in the presence of surface water foulants. *Desalination*, **13** (2), 105–220.

146. Aritomi, T. and M. Kawashima, Ion-exchange membrane. US Patent 6830671 B2, Editor 2004, Tokuyama Corporation, Japan. pp. 1–14.

147. Bae, T.-H. and Tak, T.-M. (2005) Preparation of TiO_2 self-assembled polymeric nanocomposite membranes and examination of their fouling mitigation effects in a membrane bioreactor system. *J. Membr. Sci.*, **266** (1–2), 1–5.

148. Bae, T.-H., Kim, I.-C., and Tak, T.-M. (2006) Preparation and characterization of fouling-resistant TiO_2 self-assembled nanocomposite membranes. *J. Membr. Sci.*, **275**, 1–5.

149. Liu, Y., Wang, A., and Claus, R. (1997) Molecular self-assembly of TiO_2/polymer nanocomposite films. *J. Phys. Chem. B*, **101**, 1385–1388.

150. Younos, T. and Tulou, K.E. (2005) Energy needs, consumption and sources. *J. Contemp. Water Res. Educ.*, **132**, 27–38.

151. Semiat, R. (2000) Desalination: present and future. *Water International*, **25**, 54–65.

152. Xu, T. and Huang, C. (2008) Electrodialysis-based separation technologies: a critical review. *Am. Inst. Chem. Eng.*, **54**, 3146–3159.

153. Koprivnjak, J.F., Perdue, E.M., and Pfromm, P.H. (2006) Coupling reverse osmosis with electrodialysis to isolate natural organic matter from fresh waters. *Water Res.*, **40**, 3385–3392.

154. Van der Bruggen, B. *et al.*, (2003) Electrodialysis and nanofiltration of surface water for subsequent use as infiltration water. *Water Res.*, **37**, 3867–3874.

155. Kim, J.-O. *et al.*, (2006) Development of novel wastewater reclamation system using microfiltration with advanced new membrane material and electrodialysis. *Mater. Sci. Forum*, **510–511**, 586–589.

156. Kim, S.J. *et al.*, (2010) Direct seawater desalination by ion concentration polarization. *Nat. Nanotechnol.*, **5**, 297–301.

157. Shannon, M.A. (2010) Water desalination: fresh for less. *Nat. Nanotechnol.*, **5**, 248–250.

158. Walha, K. *et al.*, (2007) Brackish groundwater treatment by nanofiltration, reverse osmosis and electrodialysis in Tunisia: performance and cost comparison. *Desalination*, **207**, 95–106.

159. Tansel, B. *et al.*, (2006) Significance of hydrated radius and hydration shells on ionic permeability during nanofiltration in dead end and cross flow modes. *Sep. Purif. Technol.*, **51**, 40–47.